



Research papers

Modelling the future impacts of climate and land-use change on suspended sediment transport in the River Thames (UK)



Gianbattista Bussi^{a,*}, Simon J. Dadson^a, Christel Prudhomme^{b,c}, Paul G. Whitehead^a

^a School of Geography and the Environment, University of Oxford, South Parks Road, OX1 3QY Oxford, UK

^b Centre for Ecology and Hydrology (CEH), Benson Lane, Crowmarsh Gifford, OX10 8BB Wallingford, UK

^c Department of Geography, Loughborough University, Loughborough LE11 3TU, UK

ARTICLE INFO

Article history:

Received 5 July 2016

Received in revised form 23 August 2016

Accepted 2 September 2016

Available online 4 September 2016

This manuscript was handled by K. Georgakakos, Editor-in-Chief, with the assistance of Joanna Crowe Curran, Associate Editor

Keywords:

Sediment transport

Climate change

Land-use change

INCA model

River Thames

Scenario-neutral approach

ABSTRACT

The effects of climate change and variability on river flows have been widely studied. However the impacts of such changes on sediment transport have received comparatively little attention. In part this is because modelling sediment production and transport processes introduces additional uncertainty, but it also results from the fact that, alongside the climate change signal, there have been and are projected to be significant changes in land cover which strongly affect sediment-related processes. Here we assess the impact of a range of climatic variations and land covers on the River Thames catchment (UK). We first calculate a response of the system to climatic stressors (average precipitation, average temperature and increase in extreme precipitation) and land-cover stressors (change in the extent of arable land). To do this we use an ensemble of INCA hydrological and sediment behavioural models. The resulting system response, which reveals the nature of interactions between the driving factors, is then compared with climate projections originating from the UKCP09 assessment (UK Climate Projections 2009) to evaluate the likelihood of the range of projected outcomes. The results show that climate and land cover each exert an individual control on sediment transport. Their effects vary depending on the land use and on the level of projected climate change. The suspended sediment yield of the River Thames in its lowermost reach is expected to change by -4% (-16% to $+13\%$, confidence interval, $p = 0.95$) under the A1FI emission scenario for the 2030s, although these figures could be substantially altered by an increase in extreme precipitation, which could raise the suspended sediment yield up to an additional $+10\%$. A 70% increase in the extension of the arable land is projected to increase sediment yield by around 12% in the lowland reaches. A 50% reduction is projected to decrease sediment yield by around 13% .

© 2016 The Authors. Published by Elsevier B.V. This is an open access article under the CC BY license (<http://creativecommons.org/licenses/by/4.0/>).

1. Introduction

Climate change is expected to alter soil erosion and sediment transport processes, although the extent and magnitude of these variations are poorly understood (Peizhen et al., 2001; Pruski and Nearing, 2002). According to Nearing et al. (2004), changes in precipitation and temperature and their interactions with land use and vegetation cover are the main climate change-related stressors that are likely to affect sediment transport in the future. These factors are expected to alter sediment production and soil loss, as well as in-channel mobilisation of sediment, phosphorus and contaminants (Mullan et al., 2012). For example, sediment transport is strongly affected by extreme precipitation and river discharge, owing to the non-linear relation between water discharge and

sediment transport rate (e.g., Julien, 2010). In many catchments, short and intense precipitation events are responsible for a large part of the total sediment transport (González-Hidalgo et al., 2010, 2013). Climate models predict a change in the behaviour of precipitation extremes. For the UK, extreme precipitation is forecast to increase in the next decades (Fowler et al., 2010; Palmer and Räisänen, 2002). Its impact on soil erosion has been assessed, for example, by Boardman (2015) and Burt et al. (2015), who detected an upward trend in average rainfall per rain day in southern England which could increase soil erosion.

Land cover changes also impact soil erosion and sediment mobilisation processes (Blöschl et al., 2007; Turner et al., 2007). Land use and land management are themselves also changing, mainly due to human interventions (Buendia et al., 2015; Evans et al., 2015; Rodríguez-Lloveras et al., 2016, 2015), but also as a result of the indirect effects of climate and other human-induced environmental changes (Mullan et al., 2012). For example, soil

* Corresponding author.

E-mail address: gianbattista.bussi@ouce.ox.ac.uk (G. Bussi).

erosion in South Eastern England has been largely affected by the shift from grassland to arable land in the second half of the 20th century, due to mechanisation and intensification of agriculture (Boardman, 2003; Howden et al., 2013).

While the impacts of climate change on sediment transport are increasingly reported in the literature (e.g., Cerdà, 1998; Foster et al., 2012; Zhao et al., 2013), only a few studies have also considered simultaneous changes in land-use and land management (de Vente et al., 2013). This has been done in the literature by a scenario-type analysis (Mullan et al., 2012), where plausible future land-use scenarios were hypothesised and used to alter the model parameterisation under different climatic conditions (see for example Nunes et al., 2009). Furthermore, there is large uncertainty about the forecasted effect of climate change on sediment transport, given that previous studies have demonstrated that different emission scenarios can lead to opposite results (Bussi et al., 2014a). The effects of both climate change and land-use change on soil erosion and sediment transport should be analysed simultaneously, as they can have important synergistic or antagonistic effects. Eventual mitigation measures based on land management and land-use change, such as reduction of arable land, extension of forested areas and introduction of better agricultural practices (Haines-Young et al., 2014), must also be evaluated under the framework of climate change to assess their effectiveness and cost.

In order to analyse the non-linear interactions between climate-driven processes that affect sediment transport at the catchment scale, hydrological and sediment models have typically been used along with climate projections from global circulation models and regional climate models (e.g., Nearing et al., 2005; Ito, 2007; and Mouri, 2015). In these approaches, climate model outputs (mainly precipitation and temperature series) obtained under specific greenhouse gas emissions scenarios are used to drive regional or catchment-scale mathematical models, which in turn provide predictions of the variable of interest (e.g., water or sediment discharge) under the climatic scenarios considered. In the field of soil erosion and sediment transport research, this approach was used recently in Nunes et al. (2009), Coulthard et al. (2012), Bangash et al. (2013), Mullan (2013), Bussi et al. (2014), Routschek et al. (2014), Francipane et al. (2015), Paroissien et al. (2015) and Simonneaux et al. (2015). As mentioned before, some of these studies also incorporated an analysis of the system response to different land-cover scenarios. The majority of these studies found a strong dependence on the climatic scenario concerned, with the different sensitivity of the response depending on combinations of climate and land-cover (Mullan, 2013; Nunes et al., 2009). Some of them also found that climate change-induced land-use change and soil management exert a larger control on soil erosion rates than climate variability (Routschek et al., 2014).

Here we employ an alternative, scenario-neutral approach, which is based on the definition of relevant climatic stressors that affect the variable of interest to quantify the joint effect of climate change and land-use change whilst at the same time evaluating uncertainty associated with the choice of climate scenario. These climatic stressors – potentially including, for example, average temperature and precipitation, precipitation intensity, seasonality and the occurrence of extremes – are perturbed within a Monte Carlo framework to establish the sensitivity of the model's outcomes to their variation. The framework is designed explicitly to quantify interactions between climatic variables and land use. The model results then form a response surface which can be compared with changes predicted using climate models. Recent applications of this scenario neutral method within hydrology, water resources and water quality research are reported by Bastola et al. (2011), Fronzek et al. (2011), Wetterhall et al. (2011), Brown et al. (2012), Brown and Wilby (2012), Prudhomme et al.

(2013), Poff et al. (2015), Prudhomme et al. (2015) and Bussi et al. (2016). The scenario-neutral methodology has some important advantages for sediment-oriented studies. For example, it allows exploration of the system's resilience to the full range of possible climate scenarios independently from individual climate modelling results. This can be very important in sediment transport studies as it enables to highlight the climate drivers associated with critical thresholds in the system, due to the non-linearity of the processes. Such thresholds might not appear when using a conventional top-down approach if the drivers are outside the range of available climate change projections. The response surface also acts as a tool for decision-makers that can be used to explore a wide range of possible sensitivities within the system to guide low- or no-regrets adaptation measures.

In this paper we assess the effects of climate change and land-use change on the sediment transport of the River Thames (UK), which has tangible value for human water consumption, for the ecosystem and for conservation. We present an extension of the scenario-neutral methodology which accounts for the joint effects of different climatic stressors and land-use scenario. Using the hydrological and water quality model INCA (Whitehead et al., 1998a; Lázár et al., 2010) we quantify the response of the specific suspended sediment yield (SSY; i.e. the average mass of suspended sediment transported over a year per unit area) to changes in annual average precipitation, extreme precipitation and annual average temperature. This analysis is repeated under four different scenarios of land use: current land use, a future scenario describing an expansion in arable land (Castellazzi et al., 2010; Crossman et al., 2013), a future scenario considering a substantial reduction in the arable land (–50%) and a theoretical scenario of total agriculture abandonment. The resulting response surfaces are compared with future climatic scenarios (Murphy et al., 2007) to establish the likelihood of changes of different magnitudes and to test the hypothesis that climate and land-cover changes exert a joint control on soil erosion and sediment transport.

In this study, we intend to propose a new methodological approach based on the scenario-neutral methodology, which can be used to quantify the impact of land-use change under different climatic scenarios, taking into account the model parametric uncertainty. Using this novel tool, we address the following research questions:

- (i) What climatic variable(s) exert the strongest control on soil erosion and sediment transport in the River Thames catchment?
- (ii) What are the interactions and feedbacks between different climatic variables and land use and what is their effect on sediment transport?
- (iii) What is the role and extent of land-use change in affecting sediment transport under a changing climate and how can it be used to contrast sediment transport?

2. Study area

2.1. The Thames catchment

The study area of this paper is the River Thames (Figs. 1 and 9, 927 km²), located in southern England and draining toward the city of London. Its water is used for freshwater supply to fourteen million people (Whitehead et al., 2013) and its non-tidal section (upstream of Teddington Weir) receives treated wastewater from approximately three million inhabitants (Kinniburgh and Barnett, 2009). The climate of the River Thames catchment is temperate with both Atlantic and continental influences. The annual precipitation is 730 mm per year (calculated between 1985 and 2014, with a minimum of 545 mm in the year

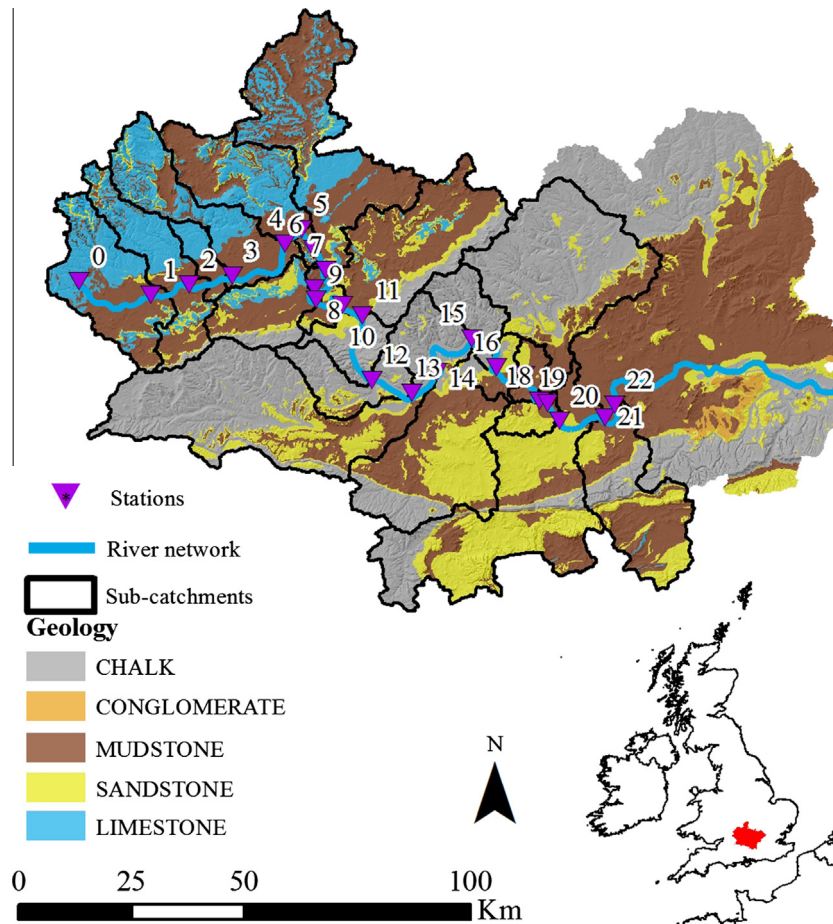


Fig. 1. Location and characteristics of the River Thames (UK). The geological map is a simplified version of the 1:50,000 geology map of England by the British Geological Survey (Smith, 2013).

1996 and a maximum of 950 mm in the year 2000) and the average temperature is 10.7 °C (between 1985 and 2014, minimum: 9.3 °C in 1986, maximum 12.1 °C in 2014), with a difference of around 2 °C between the uplands and the lowlands. The average flow is $67 \text{ m}^3 \text{ s}^{-1}$ (20–115 $\text{m}^3 \text{ s}^{-1}$), with a Q95 of $206 \text{ m}^3 \text{ s}^{-1}$. High flows usually occur in winter to early spring and low flows in summer to late autumn. The geology of the catchment is dominated by a chalk strip that crosses the catchment in its central part from east to west. The headwaters are composed predominantly of limestone, and clay/mudstone and sandstone are also present both upstream and downstream of the chalk strip (Bloomfield et al., 2011). The catchment is characterised by arable land use in its upper part (around 80% of the catchment draining to reach 4 in Fig. 1 is dedicated to agriculture and grassland), with little urban land in the headwaters but with intensively urbanised areas in the lowlands. A non-trivial fraction of the catchment is covered by forest (13% of the catchment drained by reach 19 in Fig. 1).

2.2. Data

Meteorological inputs for the hydrological and water quality model, consisting of daily precipitation and temperature time series, were obtained from the UK Met Office (Met Office, 2012). The daily precipitation, minimum temperature and maximum temperature from all the available stations within the Thames catchment were interpolated on a $5 \times 5 \text{ km}$ grid using the Thiessen polygon method, and then the daily average precipitation and temperature series were computed and used as model input. Land cover data were obtained from Fuller et al. (2002). For the hydrological

sub-model model calibration and validation, records of continuous daily water discharge at the downstream section of three of the four INCA reaches were obtained from the National River Flow Archive (NRFA, ceh.ac.uk/data/nrfa/). The sediment sub-model was calibrated using different datasets, including weekly observations of suspended sediment concentration from the Thames Initiative research platform dataset (Bowes et al., 2012), collected by the UK Centre of Ecology and Hydrology (CEH). The suspended concentration was measured by collecting a single water sample for each measurement. The samples were collected using a suspended sediment sampler, positioning the sampler intake around the 60% of the river depth (when possible). The samples were then stored in plastic bottles and subsequently taken to the laboratory. The laboratory analysis was carried out by filtering the sample through microfibre filters. The papers were then dried, weighed, and suspended solid concentrations were calculated. The suspended sediment sample were collected with a weekly frequency, from March 2009 until May 2014, in six stations along the main stem of the River Thames, corresponding with the stations 1, 3, 4, 11, 13 and 19. The samples were collected regardless of the stage, flow or season.

3. Methodology

3.1. The INCA model

In this study, the INCA hydrological and water quality model was employed to reproduce the water and sediment dynamics of the River Thames (UK). The INCA model was initially developed

as a nitrogen (Whitehead et al., 1998a) and phosphorus (Wade et al., 2002b) model, although several other sub-models were added later, such as a soil erosion and sediment transport sub-model (Lázár et al., 2010). The hydrological and water quality sub-models of INCA have been applied to several basins across the UK and Europe, and, in particular, to the River Thames catchment (Bussi et al., 2016; Crossman et al., 2013; Jin et al., 2012; Lu et al., 2016; Whitehead et al., 2015b, 2013). INCA is a semi-distributed process-based model which simulates the transformation of rainfall into runoff and the propagation of water through a river network (Wade et al., 2002a). Its inputs are daily time series of precipitation, temperature, hydrologically effective rainfall, and soil moisture deficit. The latter two are estimated using another semi-distributed hydrological model, called PERSiST (Futter et al., 2014). PERSiST is a semi-distributed catchment-scale rainfall-runoff model which is specifically designed to provide input series for the INCA family of models. It is based on a user-specified number of linear reservoirs which can be used to represent different hydrological processes, such as snow melting, direct runoff generation, soil storage, aquifer storage and stream network movement. The description of its application to the river Thames can be found in Futter et al. (2014).

The sediment sub-model of INCA has been used in several studies with focus on soil erosion and sediment transport (Farkas et al., 2013; Jarritt and Lawrence, 2007, 2006; Lázár et al., 2010; Rankinen et al., 2010; Whitehead et al., 2010). It is also a component of the phosphorus, carbon, pathogen and organic contaminant versions of the INCA model, due to absorption processes and interaction with bed sediments (Crossman et al., 2013; Futter et al., 2007; Lu et al., 2016; Nizzetto et al., 2016; Wade et al., 2002b; Whitehead et al., 2015b). A sensitivity/uncertainty analysis of its structure can be found in Jackson-Blake and Starrfelt (2015). This model was selected because of its simple structure and relatively low data demands, but also because of the large number of previous applications in the study area and in other catchments. It is structured in two parts: the land-phase model, which simulates the soil erosion and sediment production and transport processes on the hillslopes, and the in-stream compartment, which reproduces the processes and storage within the river reaches. In the land-phase model (Jarritt and Lawrence, 2007), the sediment production is caused by splash detachment, sheet erosion and rill erosion. Soil is eroded from an unlimited pool of parental material and driven to a pool of readily available sediment. The splash detachment (S_{SP} , $\text{kg km}^{-2} \text{day}^{-1}$) is estimated as in Eq. (1):

$$S_{SP} = c_{x1} p (E_{SP})^{\left(\frac{10}{10-v}\right)} \cdot 8.64 \cdot 10^{10} \quad (1)$$

S_{SP} is function of precipitation (p , mm), a soil-specific erosion potential parameter (E_{SP} , $\text{kg m}^{-2} \text{s}^{-1}$), a vegetation cover index (v , -) and a scaling parameter (c_{x1}). Analogously, the net detachment due to flow erosion (sheet and rill erosion) is calculated depending on another soil-specific erosion potential parameter (E_{FL} , $\text{kg m}^{-2} \text{s}^{-1}$), following a similar formulation but depending on direct runoff (q_{DR} , $\text{m}^3 \text{s}^{-1} \text{km}^{-2}$) rather than precipitation. A function K is defined as follows (Eq. (2)):

$$K = a_1 E_{FL} \left(\frac{A q_{DR}}{L} - a_2 \right)^{a_3} \cdot 86,400 \quad (2)$$

where a_1 , a_2 and a_3 are calibration parameters (s m^{-1} , $\text{m}^2 \text{s}^{-1}$ and non-dimensional), A the catchment area (km^2) and L the reach length (m). q_{DR} is used to simulate rill formation due to intense rainfall and runoff and can be set to a different value depending on the land use, in order to activate rill erosion where it is important (arable lands) and deactivated where the vegetation cover does not allow rill formation.

Then the flow erosion (S_{FL} , $\text{kg km}^{-2} \text{day}^{-1}$) is defined as follows (Eq. (3)):

$$S_{FL} = \frac{K(S_{TC} - S_{SP})}{(S_{TC} + K)} \quad (3)$$

where S_{TC} ($\text{kg km}^{-2} \text{day}^{-1}$) is the maximum overland flow sediment transport capacity (i.e. the maximum amount of material that can be transported from the land-phase to the stream). This is estimated depending on the catchment characteristics and the direct runoff (Eq. (4)):

$$S_{TC} = a_4 \left(\frac{A q_{DR}}{L} - a_5 \right)^{a_6} \cdot 86,400 \quad (4)$$

where a_4 , a_5 and a_6 are calibration parameters ($\text{kg m}^{-2} \text{km}^{-2}$, $\text{m}^2 \text{s}^{-1}$ and non-dimensional, respectively). The mass of sediment transported to the reach depends on the availability of readily available sediment and the overland flow transport capacity. Erosion by other sources, such as farm tracks, is not explicitly considered, although it is reasonable to assume that it is included in the parameterisation of arable areas, if the model is correctly calibrated. Soil crusting is also not included in the INCA model conceptualisation.

The suspended sediment then enters the stream via surface runoff. The transport capacity of the flow is used to separate this material into deposited and suspended material and to route the suspended part towards downstream. Most of the existing sediment models are based on similar transport capacity/material availability concepts (Aksoy and Kavvas, 2005; Bussi et al., 2013). Depending on the size of the sediment and the turbulence of the river, sediment begins to settle to the river bed and accumulate. At the same time, in-stream flows entrain settled sediment, depending on the availability and the transport capacity. Five categories of grain size are considered: clay (0–0.002 mm), silt (0.002–0.06 mm), fine sand (0.06–0.2 mm), medium sand (0.2–0.6 mm), and coarse sand (0.6–2 mm). The river shear velocity, computed depending on water depth, slope and a calibration parameter (a_7 , -), is used to determine the maximum entrainable grain size. This maximum grain size is used to estimate the proportion of each size class that can be potentially entrained from the bed sediment mass. Effective entrainment of each sediment class is calculated using Bagnold (1966) stream power equation (Eq. (5)), which is widely known and used in similar applications:

$$\omega = \rho_f g d v s = \rho_f g \frac{Q}{W} s \quad (5)$$

where ω is the stream power per unit area of bed ($\text{J s}^{-1} \text{m}^{-2}$), ρ_f is the density of water (kg m^{-3}), g the gravitational acceleration (m s^{-2}), v is the flow velocity (m s^{-1}), s is the channel slope (-), Q is the water discharge ($\text{m}^3 \text{s}^{-1}$) and W is the channel width (m). The effective entrainment (m_{ent} , $\text{kg m}^{-2} \text{s}^{-1}$) is calculated as follows (Eq. (6)):

$$m_{ent} = a_8 m_{bed} M_{PROP} \omega f \cdot 86,400 \quad (6)$$

where m_{bed} is the bed mass per unit area (kg m^{-2}), M_{PROP} is the proportion of grain size class that can be entrained (-), f a friction factor (-) calculated as the ratio of the actual hydraulic radius and the maximum hydraulic radius of a channel with the same width and a_8 a calibration parameter (entrainment coefficient, $\text{s}^2 \text{kg}^{-1}$). In the river channel, sediment settles to the river bed and accumulates, depending on the size of the sediment and the turbulence of the river. At the same time, in-stream flows mobilise settled sediment. These equations allow taking into account in-channel processes such as deposition, storage and re-entrainment. Background release of material from gullies and channels is also taken into account as a non-linear function of the river discharge depending on a calibrated coefficient (release scaling factor, a_9 ,

$\text{kg m}^{-1} \text{m}^{-3}$) and a calibrated exponent (release non-linear coefficient, a_{10} , non-dimensional).

The model can be calibrated by adjusting its parameters (Lázár et al., 2010). Some of the most influential hydrological model parameters are the direct runoff, soil water and groundwater residence times, which control the hydrological response of the catchment (i.e., the overland flow, sub-superficial flow and base flow velocities), the maximum soil moisture deficit (see Whitehead et al., 1998b) and the flow routing parameters (a , coefficient and b , exponent, used to calculate flow velocity in the river channel, see Whitehead et al., 1998b). The model also has several sediment parameters. For example, the sediment production is controlled by the splash and flow erosion potential parameters (E_{SP} in Eq. (1) and E_{FL} in Eq. (2)), the splash erosion scaling parameter (c_{x1} in Eq. (1)) and the flow erosion calibration parameters (a_1 , a_2 and a_3 in Eq. (2)). The transport of material from the hillslope to the channel network is controlled by the transport capacity calibration coefficients (a_4 , a_5 and a_6 in Eq. (3)). The sediment transport and deposition in the river channel is controlled by the shear velocity coefficient (a_7), the entrainment coefficient (a_8 in Eq. (6)) and two background release calibration coefficients (a_9 and a_{10}).

The INCA model has already been applied to the River Thames catchment (Crossman et al., 2013; Jin et al., 2012; Lu et al., 2016; Whitehead et al., 2015b, 2013). In this study, the same model structure is proposed, where the catchment is divided into 22 sub-catchments and the river into 22 corresponding reaches. For each of them, different parameters are considered. For example, topography is considered through the average slope of the sub-catchment and the slope of the channels, sub-catchment shape is considered through the use of the ratio between area and length, soil texture is considered as an input parameter, variable depending on the sub-catchment and on the land use (and it is then used to separate the material routed to the channel network into different size classes) and geology is taken into account by employing different base flow index values depending on the sub-catchment. The following land-use categories were considered: urban, arable, grassland and pasture, wetlands and forest land.

3.2. Model general sensitivity analysis

A general sensitivity analysis was applied to the INCA model of the River Thames (Spear and Hornberger, 1980; Whitehead et al., 2015a). Following a preliminary sensitivity analysis, and based on the modeller's knowledge, the following parameters were selected as the most influential and the sensitivity of the model results to them was analysed: direct runoff, soil water and ground water residence times, rainfall excess proportion, maximum infiltration rate, flow-velocity coefficient, flow threshold for saturation excess direct runoff, flow erosion direct runoff threshold (q_{DR}), splash detachment soil erodibility parameter (E_{SP}), flow erosion soil erodibility parameter (E_{FL}), transport capacity scaling factor (a_1), transport capacity non-linear coefficient (a_3), channel entrainment coefficient (a_8), release scaling factor (a_9) and release non-linear coefficient (a_{10}). E_{SP} , E_{FL} and q_{DR} are land-use-specific, although some expert knowledge-based rules were set to constrain their values, such as for example that E_{SP} and E_{FL} for arable land must be greater than E_{SP} and E_{FL} for grassland. The ranges of variation of the model parameters were also based on the modeller's knowledge previous studies (Lázár et al., 2010; Whitehead et al., 2010), although they were kept reasonably broad. The feasible space of model parameters was sampled randomly, and 10,000 different parameter sets were generated. Subsequently, the INCA model was run with each of these parameter sets, and its performance was assessed based on observed values of flow and sediment at two stations (reach 4 and reach 19), using data from 2010 to 2014. The metric used for model assessment was the Nash

and Sutcliffe Efficiency (NSE - Nash and Sutcliffe, 1970). Thresholds of NSE values were used to split the 10,000 parameter sets into behavioural and non-behavioural (Spear and Hornberger, 1980). In particular, a threshold of 0.6 for the flow and a threshold of 0.1 for the suspended sediment concentration were used. Following the model evaluation guidelines of Moriasi et al. (2007), the flow threshold corresponds to a "good" model performance. The selected behavioural models were used in the rest of the study, providing ensemble results of flow and suspended sediment concentration.

3.3. Scenario-neutral methodology for climate change analysis

In contrast with top-down approaches to climate change studies, which use climate model outputs to drive hydrological and environmental models, the scenario-neutral method takes a bottom-up approach in which vulnerability ranges of a given hydrological or environmental indicator are defined. A response surface is then produced which depicts the changes in the relevant indicator subject to the range of climatic and other environmental changes under consideration (Singh et al., 2014). The likelihood of these changes is assessed by integrating information about future climate into the results of this methodology (Prudhomme et al., 2010). A schematic diagram showing the method used in this study is given in Fig. 2. First, the climatic stressors most likely to impact SSY were identified. Plausible changes in these climatic stressors, described in Section 3.4, were then applied to the current climatic observed series of daily precipitation and temperature from 1999 to 2015. This allowed the creation of a large set of perturbed input time series (precipitation and temperature) which were used to drive the INCA model. The INCA model, driven with the altered time series, produced a set of time series of daily water discharge and suspended sediment concentration, corresponding to each perturbed input series from which a corresponding SSY value was calculated. This procedure was repeated using four land use and land management scenarios (baseline, increase in arable land, decrease in arable land and agriculture abandonment) described in Section 3.5.

3.4. Climatic alterations

In order to produce useful results, the choice of climatic alterations used to construct the response surface should be restricted to the main climatic stressors that affect the variable of interest, but they must also sample the full range of possible climate futures effectively (Prudhomme et al., 2010). The climatic variables which exert the strongest controls on river flow are precipitation and temperature (which governs the spatial and temporal variations of soil moisture and evapotranspiration). Suspended sediment yield is most strongly affected by precipitation and river flow, which control soil erosion and in-channel processes of sediment mobilisation and deposition (Julien, 2010). However, it is widely known that suspended sediment entrainment and transport occurs disproportionately during precipitation and flow extremes (Boardman, 2015), due to the non-linear relationship between flow and sediment transport by water (Julien and Simons, 1985) and so we also consider the effect of changes in extremes.

The projected changes in total precipitation and average temperature following the UKCP09 projection are shown in Fig. 3a for the study region. They are in the range of -20% to $+20\%$ for the annual precipitation and 0°C to $+2^\circ\text{C}$ for the temperature. However, we considered a broader set of changes (not shown in Fig. 3a): changes in average temperature between -1°C and $+6^\circ\text{C}$ and changes in precipitation between -30% and $+40\%$. In each case the range of possible changes was divided uniformly into fifteen divisions. The resulting set of 225 altered precipitation and

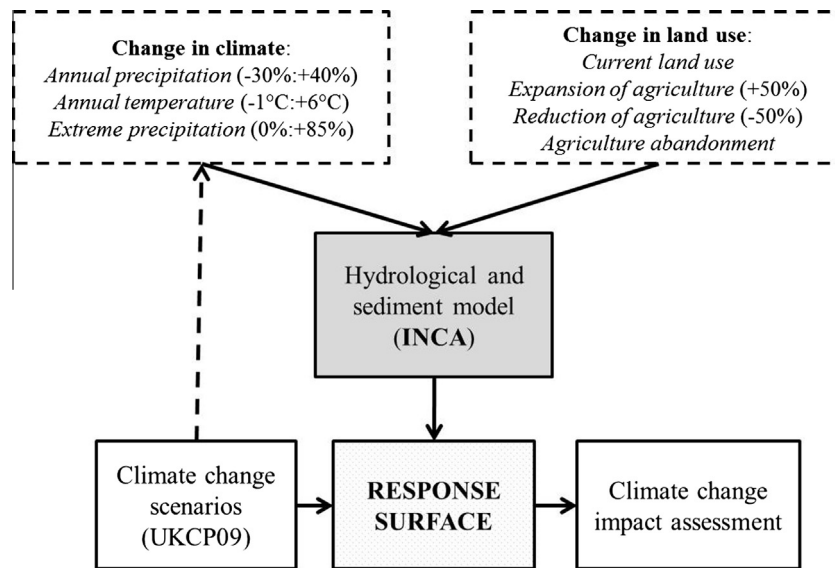


Fig. 2. Conceptual scheme of the scenario-neutral methodology.

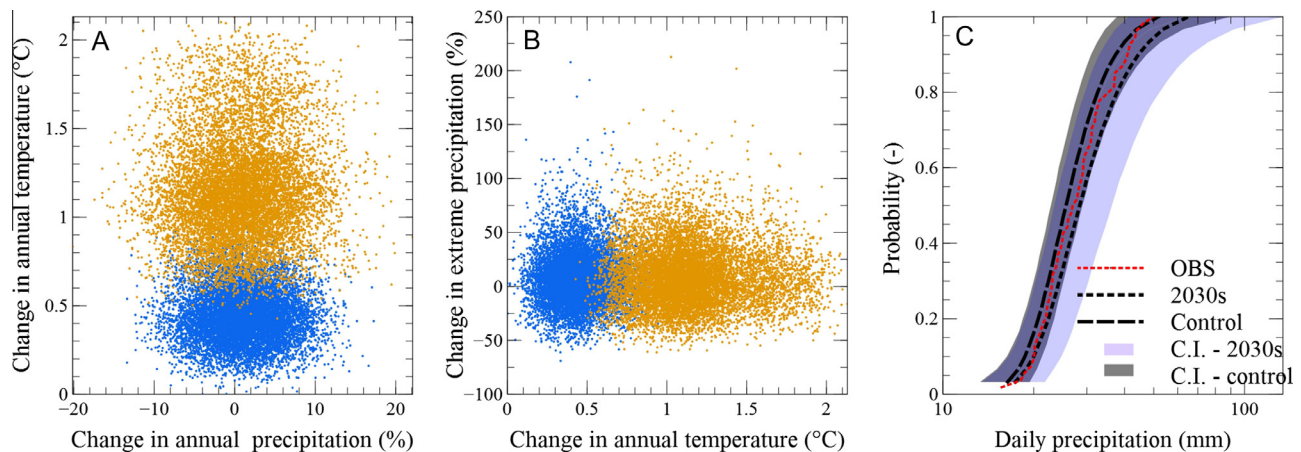


Fig. 3. (a) Change in annual temperature and annual precipitation, following UKCP09 (blue: 2030s, orange: 2050s). (b) Change in annual temperature and extreme precipitation (90% percentile of the annual maximum daily precipitation distribution function), following UKCP09 (blue: 2030s, orange: 2050s). (c) Empirical cumulative distribution functions of the annual maximum daily precipitation (C.I.: 95% confidence interval from UKCP09 projections). Control: data from UKCP09 projections for the period 1961–1990, 2030s: data from UKCP09 projections for the period 2020–2049, OBS: data from the observed precipitation and temperature series for the period 1999–2015. For visualisation purposes, the UKCP09 data were taken from 10,000 transient stochastic daily series of precipitation and temperature produced by Glenis et al. (2015). (For interpretation of the references to color in this figure legend, the reader is referred to the web version of this article.)

temperature time-series were generated by applying a uniform “delta change” transformation (Hay et al., 2000) to observed daily precipitation and temperature values accordingly.

The distribution of future changes projected by the UKCP09 probabilistic sample is given in Fig. 2b and c for the study region. As variations in extreme precipitations are not a standard product of UKCP09, these were obtained by analysing 10,000 transient stochastic daily series of precipitation and temperature produced by Glenis et al. (2015) and also used by Borgomeo et al. (2014). These are daily time series of precipitation and temperature from 1950 to 2060. Therefore, it was possible to estimate the maximum annual precipitation values for the control period (1960–1990) and for the future period (2030s and 2050s), compute an empirical cumulative distribution function for both time periods and calculate the difference. In Fig. 2b, the variations of temperature and extreme precipitation (expressed as the 90% percentile of the annual maximum daily precipitation distribution function) are depicted, following the UKCP09 over two different temporal

horizons: 2030s and 2050s. In Fig. 2c, the empirical cumulative distribution function of the annual maxima of daily precipitation (CDF) is represented, both for the control period (1961–1990, median: broken line, 95% confidence interval: grey shaded area) and for the future period (2020–2049, median: dotted line, 95% confidence interval: violet shaded area), calculated from the 10,000 climate projections from the UKCP09 as described above. A shift towards higher values of annual maximum daily precipitation is projected.

Owing to the importance of hydrological extremes events for erosion processes (Wolman and Miller, 1960; González-Hidalgo et al., 2010), changes in extreme precipitation are also considered in this study. Specifically, extreme precipitation events are defined as events with daily rainfall above 15.7 mm, which is the minimum of the annual maxima of observed daily precipitation from 1960 to 2015. The changes were implemented by altering the baseline daily precipitation time series following a transformation function based on the empirical quantile mapping approach (Déqué, 2007). In order to explore a reasonable range of alteration in extreme

precipitation values, two transformation functions were used. The two transformation functions used in this study were based on changes in extreme precipitation forecasted by the UKCP09. The first alteration, or transformation function, corresponds to a small but likely increase in extreme precipitation. Specifically, the median change forecasted by the UKCP09 was selected (e.g. a change larger than the change forecasted by 5000 out of 10,000 UKCP09 scenarios, i.e. probability = 50%). The second alteration corresponds to a larger but more unlikely shift in extreme precipitation than the first one. Specifically, a change larger than the change forecasted by 9750 out of 10,000 UKCP09 scenarios was selected (i.e., probability = 2.5%). For the sake of readability, these two extreme precipitation scenarios were called “small” and “large” increase in extreme precipitation, respectively. The two transformation functions are showed in Fig. 4 and Table 1. They are consistent with previous studies, including Fowler and Ekström (2009) who reported a change of –10% to +20% in the summer 10-day 5-year return period precipitation in South East England, and a range of 0 to +20% in winter. These transformation functions were applied on the precipitation days larger than the threshold specified above, and therefore they also alter slightly the total precipitation, by 0.9% and 4.5% respectively.

One of the limitations of the scenario-neutral methodology is the reduction of number of stressors considered for a best readability and easier interpretation (here: 2 stressors only). This means that not all climate-related stressor that affect sediment transport have been considered. Other climatic stressors exist that might vary in the future and could have an impact on SSY. For example, a change in precipitation seasonality could change the wetting and drying cycle of the soil and therefore change soil properties such as infiltration and erodibility (Cerdà, 1999, 1997), in-channel sediment storage (Bussi et al., 2014b; Collins and Walling, 2007; Duijsings, 1986; López-Tarazón et al., 2011; Piqué et al., 2014) as well as affecting river flow (Prudhomme et al., 2010). A variation in the number of rainy days also could have an effect on sediment transport, in the case of both an increase or a decrease in the number of days of precipitation (Nearing et al., 2004). However, one of the advantages of this methodology is that it allows isolating the effects of single stressors leading to conclusions that can drive decision making. Because changes in the stressors mentioned here are expected to have a secondary role compared with the effect exerted by changes in average precipitation and temperature and changes in extreme precipitation, and because the effects of drying and wetting cycles on soil crusting and soil properties are not accounted for in the modelling of sediment delivery and transport model, they were not considered in this study.

3.5. Land-use variations

In this study we considered four land cover scenarios: (i) present day land use (called “baseline” scenario); (ii) arable land expansion; (iii) arable land reduction; and (iv) agriculture abandonment. Present day land use (Fig. 5) was obtained from the UK Land Cover Map 2007 (Smith et al., 2007). The catchment headwaters are dominated by arable land, while urban and forest land uses assume more importance in the lowlands. The arable land expansion scenario was defined according to the land cover model LandSFACTS (Castellazzi et al., 2010), which focuses on crop arrangement under increasing population, considering food security as a dominant driving force for land use change. Arable conversion from other land uses was permitted only on prime land and only from areas previously identified as grasslands (Crossman et al., 2013), and resulted in an increase from 3526 km² to 5988 km² (over 9927 km² catchment area) of arable land (70% increase). This means that the portion of arable land increases from 36% to 60% for the Thames at Teddington (reach 22) (Fig. 5). This

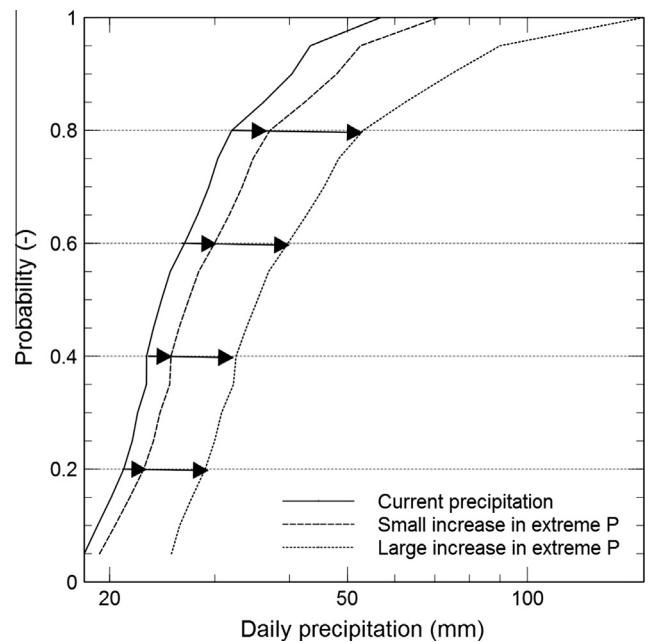


Fig. 4. Cumulative distribution functions of the three extreme precipitation scenarios considered in this study.

Table 1

Extreme precipitation transformation function. The quantile is referred to the probability of the empirical distribution function of the observed annual maximum of daily precipitation.

| Quantiles (%) | Current precipitation (mm day ⁻¹) | Small increase of extreme precipitation (%) | Large increase of extreme precipitation (%) |
|---------------|---|---|---|
| 10 | 20.0 | +6.9 | +37.2 |
| 20 | 21.9 | +8.0 | +36.9 |
| 30 | 23.1 | +9.0 | +38.2 |
| 40 | 24.8 | +9.9 | +41.2 |
| 50 | 26.9 | +11.0 | +44.8 |
| 60 | 29.2 | +12.2 | +48.9 |
| 70 | 31.1 | +13.7 | +55.9 |
| 80 | 35.5 | +15.8 | +65.9 |
| 90 | 40.9 | +18.9 | +84.6 |
| 95 | 43.5 | +21.3 | +107.7 |

scenario was introduced into the INCA model by altering the fractions of the catchment assigned to each land use. The INCA model allows runoff production, soil erosion and sediment delivery parameters to be changed depending on the land use, thus representing the effect of changing land use on sediment transport. The arable land reduction scenario was set up by reducing the arable land by 50%, increasing forest land by 20% and assigning the remaining land to grassland. This was done in order to analyse the effect of reducing the arable land as a strategy to reduce sediment export by the River Thames. The agricultural abandonment scenario was implemented by setting arable land to 0%, increasing forest land by 20% and assigning the remaining land to grassland. This theoretical scenario was considered with the aim of analysing the hypothetical sediment transport response of the catchment if it was to be returned to a more natural status. This scenario, although highly unlikely in the foreseeable future for the Thames catchment, has already taken places in other parts of the world, such as the Spanish Pyrenees (Gallart and Llorens, 2004).

The 675 simulations described above (i.e. simulations driven by all possible combinations of 15 altered precipitation time series, 15 altered temperature time series and 3 alterations of the extreme precipitation) were repeated four times, one for each land-use

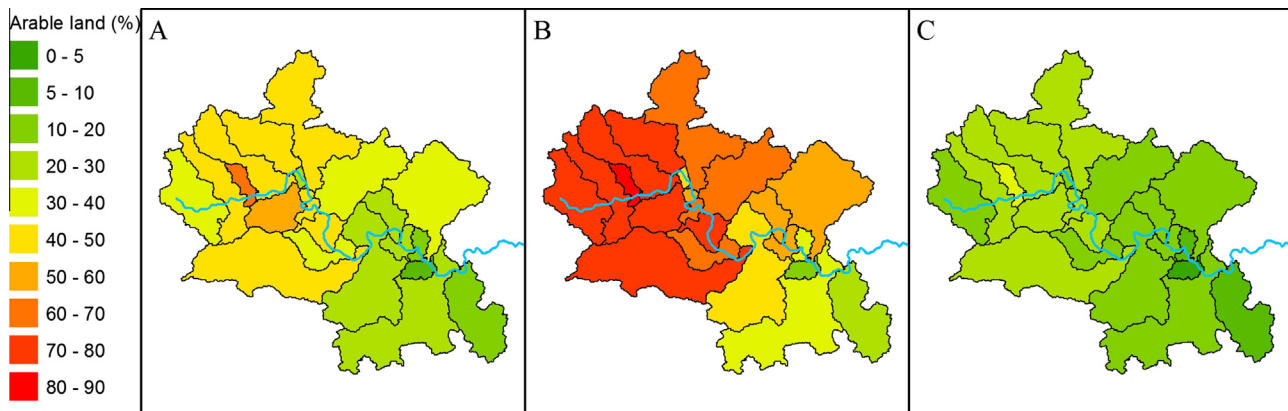


Fig. 5. Proportion of arable land: (a) baseline, (b) arable land expansion, (c) arable land reduction. The agriculture abandonment scenario is not represented.

scenario, and their results were compared to assess the net impact of land-use change on sediment transport under a changing climate.

3.6. Likelihood of predicted changes

The UKCP09 probabilistic change factor scenarios were developed by the UK Met Office to provide climate change projections of climate change over the UK with greater spatial and temporal detail than previous climate scenarios, but accounting for important uncertainties in Global Climate Models. These projections are based on the results of the HadCM3 coupled ocean-atmosphere Global Circulation model (Gordon et al., 2000), which was run as a perturbed physics ensemble to sample model and parameter uncertainties (Murphy et al., 2007). HadCM3 projections were downscaled on a 25 km grid over seven overlapping 30-yr time periods based on an ensemble of 11 variants of the regional climate model HadRM3, and a statistical procedure was applied to build local-scale distributions of changes for various climate variables. UKCP09 gives projections for each of three of the IPCC's Special Report on Emissions Scenarios (SRES) scenarios (A1FI - called High in UKCP09, A1B - Medium and B1 - Low). Among the available outputs, expected changes in average precipitation and temperature following the different emission scenarios are given (change factors). In the present study, we assess the risk of changes in SSY by comparison with climatic properties taken from a set of 10,000 change factors (Murphy et al., 2007) under the A1FI emission scenario for two temporal horizons: 2030s and 2050s. The A1FI scenario was chosen as it is the most severe scenario available, but one of the strength of the scenario-neutral methodology is that the scenario could be easily replaced without having to re-run all the simulations.

4. Results

4.1. Model implementation

The Monte Carlo general sensitivity analysis resulted in 21 behavioural models. Fig. 6 shows their results for the River Thames at the reach 4, both in terms of flow and suspended sediment concentration. The results of the sediment sub-model are also shown in Fig. 7, where the distribution functions of the observed values of suspended sediment concentration are compared to the distribution functions of the modelled values. Note that the modelled values were resampled with the same time frequency as the observed values (e.g. weekly) for consistency. The model results indicate a SSY of 0.030 (0.020–0.063) Mg ha⁻¹ yr⁻¹ for reach 19 and 0.033 (0.016–0.053) Mg ha⁻¹ yr⁻¹ for reach 4 for the period 2010–2014.

Fig. 7 also shows the spatial validation of the model. It can be observed that the results of the model at reach 1, 3, 11 and 13 (i.e. the reaches not used for behavioural model selection) are good in terms of reproduction of the observed distribution function of suspended sediment concentration. Spatial validation showed model biases of 0–27% for reach 1 and 4–65% for reach 13 regarding suspended sediment concentration.

4.2. Climate change impact under current land use

The precipitation and temperature changes considered in this study largely affect river flows, causing alterations in the average water discharge of the River Thames at reach 19 from –50% (caused by the combination of 30% reduction in precipitation and 6 °C increase in temperature) to +83% (caused by the combination of 40% increase in precipitation and 1 °C decrease in temperature). The increase in extreme precipitation considered causes a further increase of water discharge (around +1% in the case of a small increase in extreme precipitation, around +5% in the case of a large increase in extreme precipitation). The simulated SSY varies from 0.010 to 0.148 Mg ha⁻¹ yr⁻¹ for the Thames at reach 19, under uniform changes of precipitation and temperature and no increase in extreme precipitation. The small increase in extreme precipitation scenario considered in this study is responsible for an additional average increase of SSY of 2%, given the same condition of uniform precipitation and temperature change, while the large increase in extreme precipitation scenario causes an average additional SSY increase of 11%. Note that here we do not suggest that any of these changes is likely, neither that they are meteorologically plausible; we simply calculate them to be the catchment's response to such a combination of changes were they ever to occur.

Fig. 8 shows the results of the scenario-neutral methodology in terms of SSY response to climatic variations for station 4 under current land use. The top plots represent the median change in SSY and the bottom plots show the standard deviation of the change in SSY. The left-hand side plots represent the response of the system to changes in annual precipitation and temperature, with no changes in extreme precipitation, the central plots represent the response of the system to changes in annual precipitation and extreme precipitation, with no changes in annual temperature, and the right-hand side plots the response of the system to changes in annual temperature and extreme precipitation, with no changes in annual precipitation.

4.3. Climate change impact under different land use scenarios

The land-use change scenarios considered in this study have little effect on mean river flows compared to the impact of the

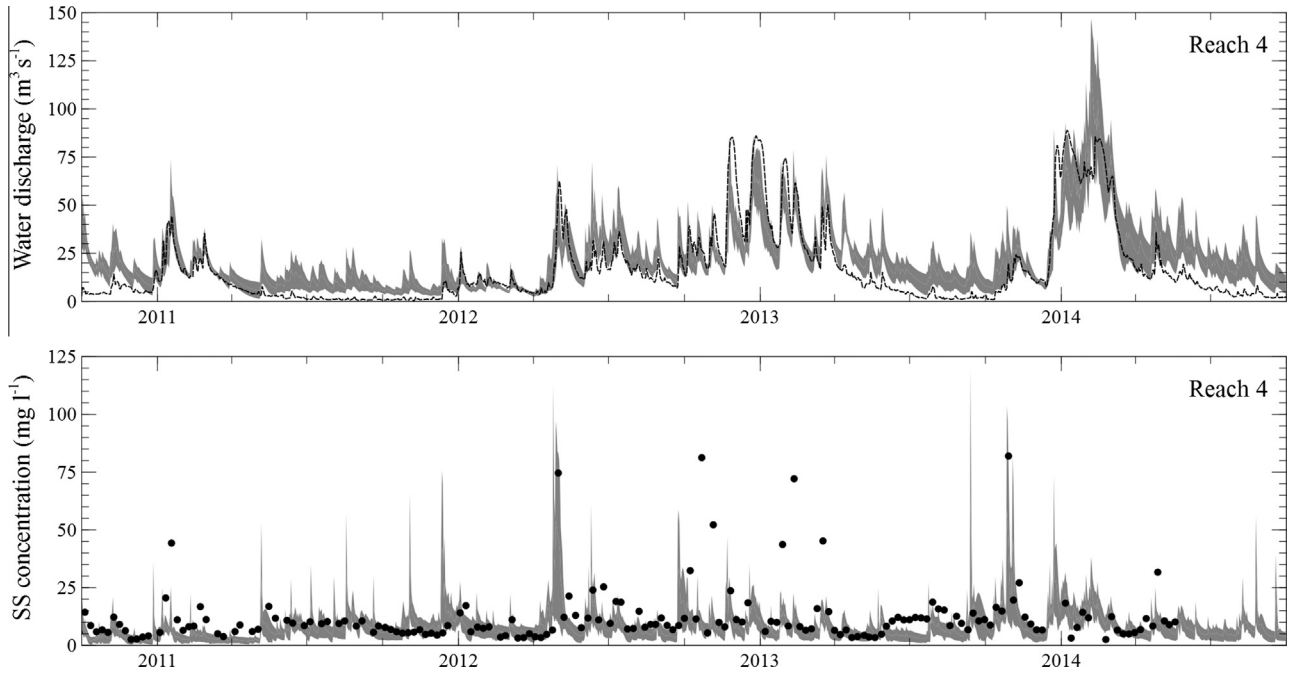


Fig. 6. Water discharge model results (comparison with water discharge records from NRFA) and suspended sediment concentration model results (comparison with suspended sediment concentration values from the Thames Initiative dataset). The black broken line is the observed water discharge, the black dots the measured suspended sediment concentration values and the grey areas the model results.

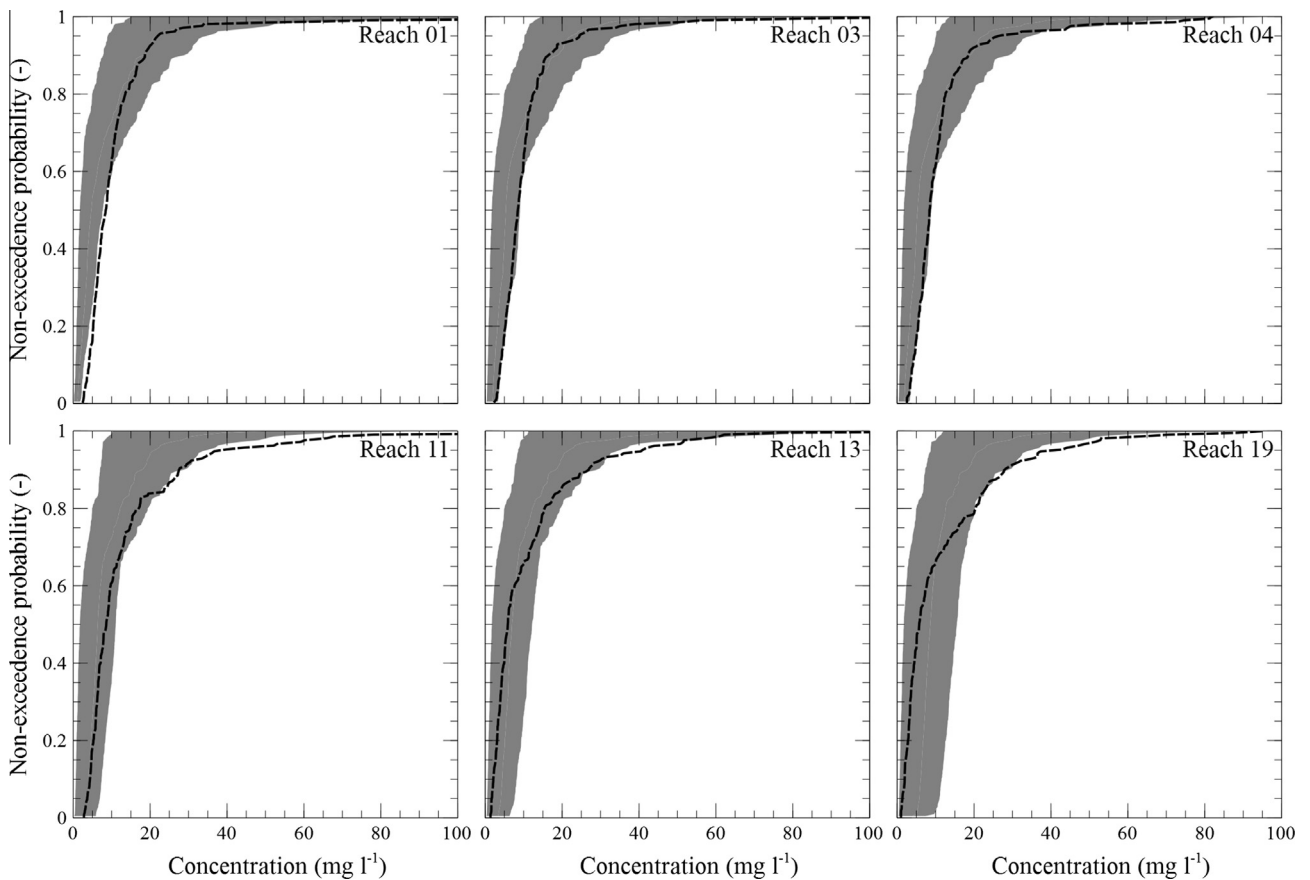


Fig. 7. Cumulative distribution functions of suspended sediment concentration. The black broken lines are the observed suspended sediment concentration distribution functions, based on the available samples, the grey areas the modelled suspended sediment concentration distribution functions.

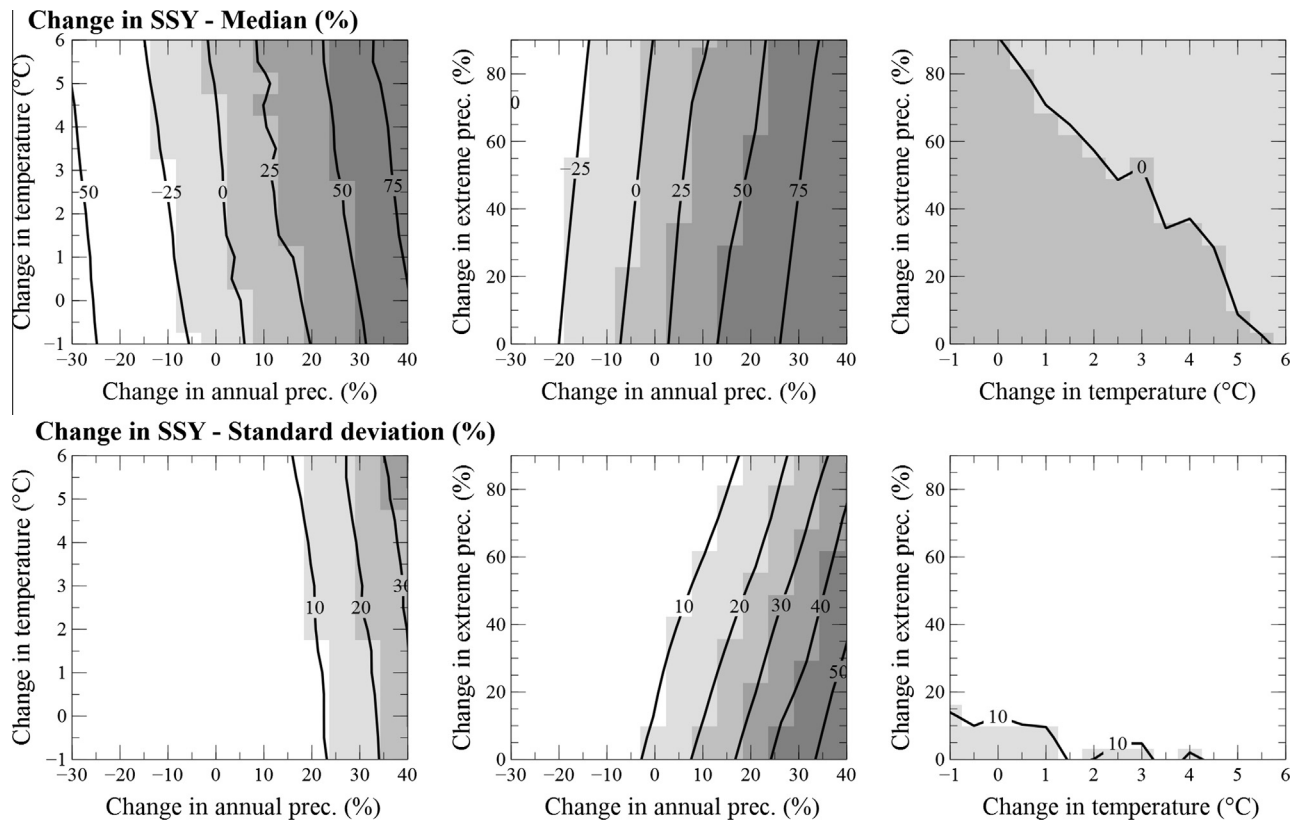


Fig. 8. Response of the system to climatic alterations. Top plots: median change in SSY change, bottom plots: standard deviation of the change in SSY.

climatic stressors, with a slight reduction in water discharge (estimated to be -0.2% by the INCA model), owing to an increase in evapotranspiration. By contrast, the impact of land-cover change on suspended sediment transport is considerable. Land-use change does not alter the pattern of the system response to changes in precipitation and temperature, but does affect the magnitude of SSY values. In Table 2, the net contribution of land-use change to the variations of SSY is shown for reach 4 and 19, i.e. the increase or decrease in SSY caused by a change in land use under the same climatic conditions. For example, for reach 4, the arable land expansion scenario, causes an average SSY increase of 41%, while under the arable land reduction scenario SSY decreases on average by -30% , and under the agriculture abandonment scenario -59% .

In Fig. 9, the joint effect of climatic change and land-use change on SSY is shown for the Thames at reach 4 (left) and reach 19 (right). These histograms describe the range and probability distribution of sediment response to a range of climate and land-use scenarios. Due to the use of a model ensemble rather than a single model, the histograms are represented as an envelop curve rather than a single line. In general, the land-use change impact is small compared with the climate change uncertainty range, but certain land-use changes can exacerbate or reduce the impact of climate change systematically. It is very important to note that there is a clear difference between the different land use management options.

4.4. Likelihood of predicted changes

The response surface plots shown above can be used for exploring combinations of climate change and land use or land management options. Nevertheless, they do not convey information about the plausibility or probability of the expected climatic changes, unless they are compared with projections from climate models

(Prudhomme et al., 2010). In this section, we analyse the response of the system to changes in average precipitation, average temperature and extreme precipitation projected by the UKCP09. The values of change in SSY depending on the land use and extreme precipitation scenarios are reported in Table 3, where the median changes and their confidence interval (computed according to the variations in average temperature and precipitation given by UKCP09 for two different future periods: 2030s and 2050s) are shown for each combination of land use and extreme precipitation change.

4.5. Effectiveness of arable land reduction

In Fig. 10, the effectiveness of the arable land reduction as a sediment transport reduction mitigation measure is assessed. In this diagram, the difference between the SSY under the baseline scenario and arable land reduction scenario is represented (in %) with different shades of colour (red¹-brown: smaller decrease in SSY, white-yellow: larger decrease in SSY). The SSY decrease is a proxy measure of the average effect of reducing arable land. Each pixel in this figure represents the effectiveness for reach 4 and reach 19 under a specific combination of change in average precipitation (in the x-axis) and increase in extreme precipitation (in the y-axis, quantified as the increase in the 90% percentile of the CDF), given a fixed increase in average temperature ($+2\text{ }^{\circ}\text{C}$). The space of combinations of changes in average precipitation vs changes in extreme precipitation following the UKCP09 is also depicted as black dots. The larger plots represent the results obtained with the median of the model ensemble, while the smaller plots are the minimum and the maximum respectively. The standard deviation of the change in SSY is

¹ For interpretation of color in Fig. 10, the reader is referred to the web version of this article.

Table 2
Net contribution of the land use change to the variation of SSY.

| Reach | Extreme precipitation increase | Arable land expansion | Arable land reduction | Agriculture abandonment |
|----------|---|-----------------------|-----------------------|-------------------------|
| Reach 4 | No increase in extreme precipitation | 41 (41–41) | –30 (–30 to 30) | –59 (–59 to 59) |
| | Small increase in extreme precipitation | 43 (43–43) | –31 (–31 to 31) | –60 (–60 to 60) |
| | Large increase in extreme precipitation | 47 (47–47) | –33 (–33 to 33) | –64 (–64 to 64) |
| Reach 19 | No increase in extreme precipitation | 20 (4–40) | –18 (–28 to 4) | –32 (–40 to 20) |
| | Small increase in extreme precipitation | 22 (6–44) | –17 (–27 to 1) | –30 (–39 to 18) |
| | Large increase in extreme precipitation | 31 (15–55) | –10 (–21 to 8) | –25 (–34 to 12) |

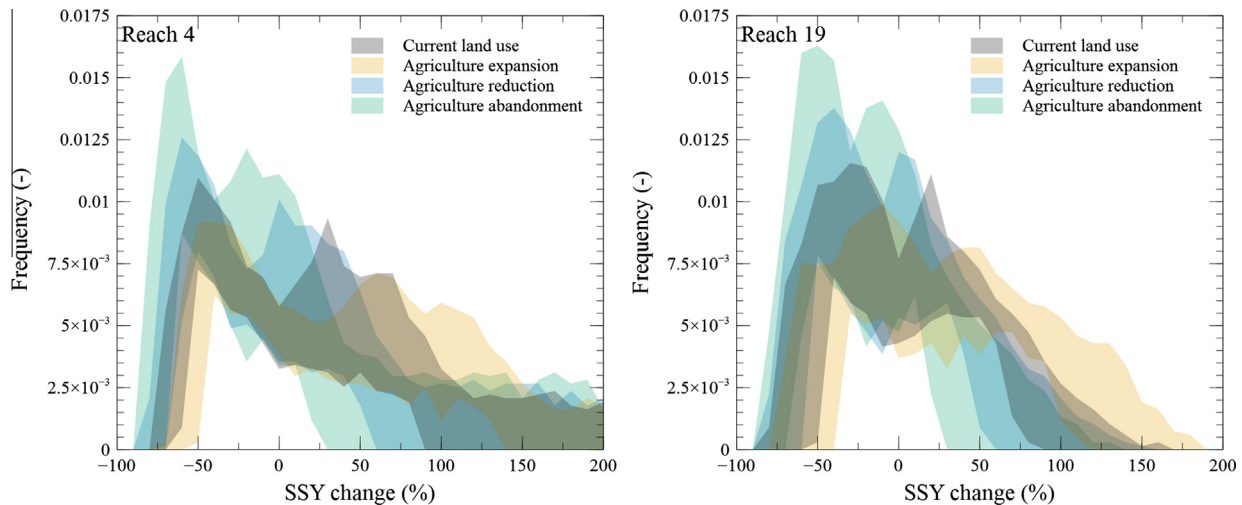


Fig. 9. Histograms (represented as empirical probability distribution functions) of the change in suspended sediment yield (SSY) at reach 4 (left) and reach 19 (right) under different land use and land management scenarios under large increase in extreme precipitation.

Table 3

Change in SSY median value and $p = 0.95$ confidence intervals (%) corresponding to precipitation and temperature changes projected by UKCP09, under different scenarios of land use and extreme precipitation increase.

| Reach | Future time slice | Extreme precipitation increase | Baseline | Arable land expansion | Arable land reduction | Agriculture abandonment |
|----------|-------------------|---|----------------|-----------------------|-----------------------|-------------------------|
| Reach 4 | 2030s | No increase in extreme precipitation | –6 (–22 to 15) | 16 (–3 to 42) | –22 (–35 to 4) | –37 (–48 to 24) |
| | | Small increase in extreme precipitation | –4 (–19 to 20) | 19 (–1 to 46) | –20 (–33 to 1) | –36 (–46 to 21) |
| | | Large increase in extreme precipitation | 7 (–10 to 32) | 32 (11–62) | –11 (–25 to 9) | –29 (–40 to 13) |
| | 2050s | No increase in extreme precipitation | –8 (–26 to 16) | 13 (–9 to 42) | –23 (–38 to 4) | –39 (–50 to 24) |
| | | Small increase in extreme precipitation | –6 (–23 to 19) | 16 (–6 to 46) | –22 (–36 to 1) | –37 (–49 to 22) |
| | | Large increase in extreme precipitation | 5 (–14 to 31) | 30 (6–61) | –13 (–28 to 9) | –31 (–43 to 14) |
| Reach 19 | 2030s | No increase in extreme precipitation | –4 (–16 to 13) | 20 (4–40) | –18 (–28 to 4) | –32 (–40 to 20) |
| | | Small increase in extreme precipitation | –2 (–14 to 16) | 22 (6–44) | –17 (–27 to 1) | –30 (–39 to 18) |
| | | Large increase in extreme precipitation | 6 (–8 to 27) | 31 (15–55) | –10 (–21 to 8) | –25 (–34 to 12) |
| | 2050s | No increase in extreme precipitation | –6 (–18 to 13) | 18 (0–40) | –19 (–30 to 4) | –32 (–42 to 20) |
| | | Small increase in extreme precipitation | –4 (–17 to 16) | 20 (2–44) | –18 (–29 to 1) | –31 (–41 to 18) |
| | | Large increase in extreme precipitation | 4 (–11 to 26) | 30 (11–55) | –11 (–24 to 8) | –26 (–36 to 12) |

represented in the bottom plots, as derived from the ensemble of models employed in this study. These two plots provide an estimation of the uncertainty affecting the land management effectiveness assessment (i.e., large standard deviation: large uncertainty, and vice versa).

5. Discussion

5.1. Model implementation

The model results, though satisfactory in terms of reproduction of the water and sediment dynamics of the River Thames catchments, reveal the presence of uncertainty in the model predictions. From Fig. 6, it can be seen that some of the highest values of

suspended sediment concentration are underestimated by the model. This could be due to processes that are not well reproduced by the model, such as localised river bank failure or erosion from farm tracks. This appears not to be a concern in the upper reaches, as shown in Fig. 7, while in the lower reaches the model tends to slightly underestimate low probability concentrations. From the perspective of this study, this is likely to affect the model representation response of the lower Thames to changes in extreme precipitation, leading to small underestimations. Nevertheless, this study is focused to estimating the impact of different stressors on suspended sediment load, which is the product of flow and suspended sediment concentration. The thresholds chosen for model selection for flow and suspended sediment concentration (NSE = 0.65 and 0.1 respectively) are well within the ranges provided by Moriasi et al. (2007), and therefore the model estimates of suspended load

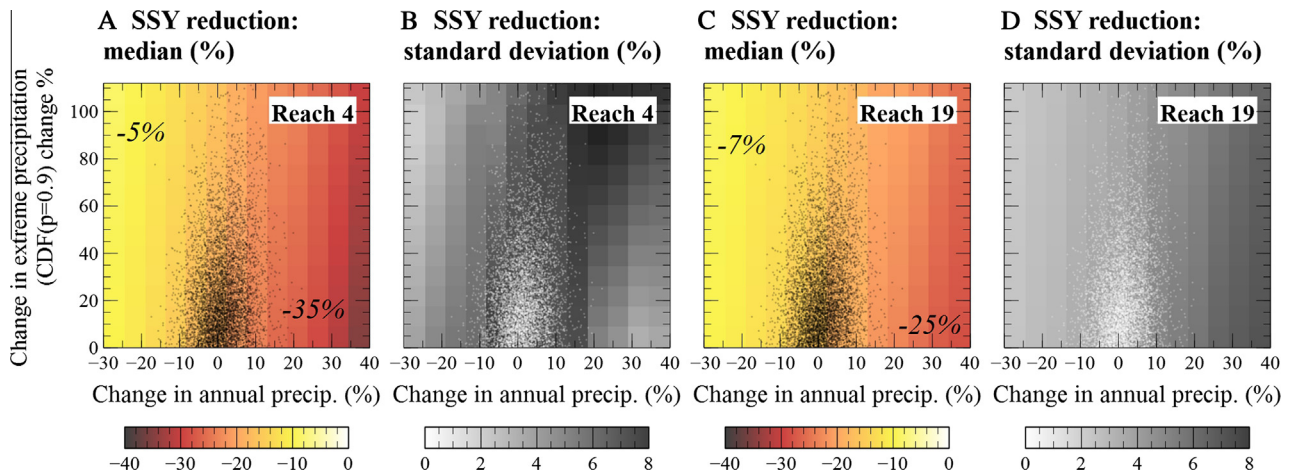


Fig. 10. Effectiveness of land management scenario (% difference between SSY change under the baseline scenario and the arable land reduction scenario). (a) Median effectiveness, reach 4; (b) standard deviation of the effectiveness, reach 4; (c) median effectiveness, reach 19; (d) standard deviation of the effectiveness, reach 19. The black dots represent UKCP09 projections for the 2050s. For visualisation purposes, the UKCP09 data were taken from 10,000 transient stochastic daily series of precipitation and temperature produced by Glenis et al. (2015).

can be considered reliable. The SSY obtained by the model is close to estimates of $0.068 \text{ Mg Ha}^{-1} \text{ y}^{-1}$ for the Thames at Days Lock (3500 km^2) by Neal et al. (2006), and lower compared with other large catchments in the UK (Worrall et al., 2013). Furthermore, the sensitivity analysis was carried out using a variety of climatic conditions, from a dry year (2010) to a very wet winter (2013–14), thus ensuring that the model is able to respond to a wide range of climatic conditions.

5.2. Climate change impact under current land use

A broad range of climatic variations was explored, to understand the effect of climatic variations not necessarily included by the available climate model projections. From the response surfaces, it can be seen that SSY increases with precipitation, due to larger soil erosion (given by both lower infiltration and increased splash erosion) and to larger river channel flow. SSY is also affected by temperature: higher temperatures increase evapotranspiration and thus decrease flow and SSY. Extreme precipitation also affects SSY, given that an increase in extreme precipitation triggers an increase in SSY. Concerning the uncertainty (standard deviation of the change in SSY, bottom plots in Fig. 8), this seems to be larger when large increase in annual precipitation are considered, while it is smaller when decrease in annual precipitation are considered. In other words, the ensemble of behavioural models used in this study tends to converge to similar results when a decrease in annual precipitation is considered, while it tends to diverge when a large increase in annual precipitation is taken into account.

Fig. 8 shows the magnitude of SSY change in response to climatic alteration and the uncertainty that affects these estimates, but it can also provide a measure of the sensitivity of the system to climatic changes. This can be interpreted by looking at the gradient of the values in the plots. For example, it can be seen that the gradient corresponding to changes in annual precipitation (x-axis of the left and central plots) is much larger than the gradient of the other two climatic variables (annual temperature and extreme precipitation). This means that, within the range of the climatic alterations considered in this study, the most influential, or dominant, is average precipitation, suggesting that the River Thames catchment has a much larger sensitivity to changes in average precipitation than to changes in extreme precipitation or temperature. There is more variability within simulations with the same temperature change than between them (and the same can be said

about extreme precipitation), meaning that temperature changes and extreme precipitation changes have second order effects compared to the effects of changes in average precipitation.

These results substantially agree with previous studies on the impact of climate change on sediment transport (e.g. Nearing et al., 2005; Pruski and Nearing, 2002), although the extent of the role played by changes in extreme precipitation is usually high uncertain. In this study, this was quantified in detail for the River Thames. It must be noted that this effect is expected to be highly local, i.e. the impact of changes in extreme precipitation is expected to vary depending on climate and location of the catchment. Even within the same catchment, different sub-catchments respond differently to climatic alterations, due to different land-use configurations. For example, a scenario with an increase of $3 \text{ }^\circ\text{C}$ and a decrease of 10% in precipitation returns a decrease of 29% in SSY for reach 4 and 20% for reach 19, and a scenario with a decrease of $1 \text{ }^\circ\text{C}$ and an increase of 20% in precipitation returns an increase of 44% SSY at reach 4 and 39% at reach 19. Similarly, a large increase in extreme precipitation causes an average increase in SSY of 14% at reach 4 and of 11% at reach 19. This is because the uplands of the River Thames are more sensitive to changes in precipitation than the lowlands, due to the larger extension of arable land in the upper sub-catchments.

5.3. Climate change impact under different land use scenarios

The impact of land-use change on water discharge is very limited and consistent with that reported by Crooks and Davies (2001). No catchment-scale studies were available regarding the impact of land-use change on the sediment transport of the River Thames, to the authors' knowledge. Land-use change appears to be a key driver of SSY alterations, although it is important to remember that both land-use change and climate change scenarios were chosen by the authors and do not indicate the likelihood of changes. It is very important to note that, despite modelling uncertainty, a strong signal of change between the different land-use options can be seen, i.e. all the behavioural models lead to the same conclusions in terms of impact of land-use change on SSY. This means that the approach proposed in the study was able to identify the effect of land use management on SSY taking into account the model uncertainty, leading to robust conclusions.

In terms of spatial variations of the effects of land-use change, Fig. 9 shows that there is a slightly different response of reach 4

(located in the upper part of the catchment) and reach 19 (located in the lower part). This is related mainly to the fraction of catchment dedicated to arable land use, and the proportion of arable land versus grassland, but it is also connected to other phenomena, such as the balance between sediment availability and sediment transport capacity of a river reach, which can be altered by changes in climate and land use. The use of a mathematical model, such as the INCA model, allows us understanding and extrapolating the extent of these non-linear interactions between different processes under conditions that have not been observed yet.

It is difficult to compare the results of this paper with previous studies, given that just a few modelling studies have been published so far about the joint impact of climate change and land-use change on sediment transport at the catchment scale. However, a few recent studies also noted that land-use change effects can be as relevant as climate change effects, especially in human-impacted catchments and agricultural areas. For example, [Parioissien et al. \(2015\)](#) found that the effect of land-use change was much more significant than the effect of precipitation change in an agricultural catchment in Southern France. [Serpa et al. \(2015\)](#) also pointed out the role of land-use changes in minimizing the indirect effects of climate changes for two catchments in Portugal and stressed the importance of an integrated approach combining the effects of climate and land-cover change for a realistic evaluation of the future state of natural resources. Similarly, [Simonneaux et al. \(2015\)](#) noted that climate changes alone might be of minor importance compared to changes in land use for an arid catchment in Morocco, especially regarding the evolution of badlands, which are closely conditioned by human actions. [Rodríguez-Lloveras et al. \(2016\)](#) showed that land-use change can counterbalance climate change for a catchment in Southern Spain. Nevertheless, these studies were conducted in more erosion-prone areas, and they might not be comparable with the River Thames. [Routschek et al. \(2014\)](#) presented a study on a temperate catchment in Germany, which led to conclude that land-use change and soil management induced played a more relevant role than climate change alone, and similar conclusions were drawn by [Mullan et al. \(2012\)](#). In the present study we show that for the River Thames the extent of climate and land-use change effect is variable depending on the sub-catchment and the river reach, and, although the climate change impact appears to be predominant at the catchment scale, the amount of arable land also controls an important part of the total sediment production and sediment transport.

Finally, it is worth mentioning that the INCA model land use and vegetation biomass parameters are static, and are not affected by intra- or inter-annual climatic variability. Therefore, the effect of climate change acting on vegetation and land use, which in turn affects sediment production, was not taken into account. Over relatively short time-scales in a heavily managed setting like southern Britain, where land cover is often not natural, the effects of this feedback were considered to be minimal. This is acknowledged as a priority for future regional-scale sediment model development ([de Vente et al., 2013](#)), although it is considered for example in the sediment transport model PESERA ([Kirkby et al., 2008](#)).

5.4. Likelihood of predicted changes

The small increase in extreme precipitation considered in this study has limited effect. On the other hand, the large increase in extreme precipitation has a very clear effect at both stations, increasing the SSY by around 13% at reach 4 and around 10% at reach 19, for the 2030s (+10% and +10% for the 2050s). These figures changes under different land-use changes scenarios: for example, under the arable land expansion scenario they are +16% and +11% respectively, for the 2030s, while under the arable land reduction scenarios they are +11% and +12%. While exploring a

broad range of climatic combination may help understanding the system response under global change, the incorporation of climate model forecasts like the UKCP09 in the scenario-neutral methodology provides policy-makers with a clear figure of what the expected changes will be. It has to be acknowledge that the uncertainty of the final results is extremely large, but the methodology described in this paper can at least account for the climate model uncertainty, by using a large set of climate model outcome like the UKCP09 product, and the hydrological model parametric uncertainty, by employing an ensemble of equifinal behavioural models rather than a single model.

5.5. Effectiveness of arable land reduction

[Fig. 10](#) shows that the reduction of arable land as a measure to reduce SSY in the Thames is effective under all the climate change scenarios considered for the Thames, with reductions of SSY ranging from 5% to –35% for reach 4 and between 7% and 25% for reach 19. The effectiveness of the arable land reduction within the area defined by the UKCP09 projections ranges between –20% and 30%. On the other hand, this plot also shows that the effectiveness of the arable land reduction may vary depending on the climate scenario. For both sub-catchments, the proposed arable land reduction is effective on a scenario of precipitation reduction (left part of the plot), but they are also effective in the case of increase in extreme precipitation. In particular, the SSY reduction is more sensitive to changes in annual precipitation rather than changes in extreme precipitation (i.e., the vertical gradient in the response surfaces is minimal compared to the horizontal gradient). [Fig. 10](#) also shows the modelling uncertainty of the results. For example, it can be see that for reach 4 the standard deviation of the SSY reduction is larger than for reach 19 in the central area of the plot, i.e., the area of climatic outcomes defined as plausible by the UKCP09. Knowing the modelling uncertainty in reproducing the system response is of paramount importance for catchment managers, as it provides an estimate of the likelihood of a given land management measure to obtain the expected results.

This plot also shows the potential of the scenario-neutral methodology for assessing a soil erosion mitigation strategy under changing climate and changing land use. Owing to the particular approach, which analyses several different combinations of climate and land use, it was possible to assess whether this strategy was robust and effective under different climatic and land-use conditions. This provides decision makers and land managers with a simple tool that might inform climate change adaptation policy. However, this was not considered in this study because the representation of soil erosion mitigation measures into the model parameterisation requires a more detailed investigation that was out of the scopes of this paper.

6. Conclusions

This paper investigated the joint control exerted by climate change and land-cover change on suspended sediment discharge in the River Thames catchment (UK), through the use of a scenario-neutral method and the UKCP09 projections ([Murphy et al., 2009](#)). The results showed that UKCP09 changes in average precipitation and average temperature are likely to cause a median reduction in the suspended sediment yield of the River Thames by 6% in the uplands and by 4% in the lowlands, although the confidence interval ($p = 0.95$) is very broad (–22% to +15% and –16% to +13% respectively), owing to the high variability in expected future precipitation and temperature. The UKCP09 projections also project an increase in extreme precipitation, which is likely to increase suspended sediment yield by up to 13% in the uplands,

potentially compensating the reduction due to changes in average precipitation and temperature (subject to the actual increase of extreme precipitation).

The main findings of this study are listed as follows:

- (i) This paper has shown a methodological approach to assess the joint impact of climate and land-use change, taking into account the climate and sediment model uncertainties and leading to robust conclusions. If used along with a climate model, this methodology can also offer a measure of the plausibility of expected changes.
- (ii) The control exerted on the soil erosion and sediment transport of the River Thames catchment by a change in average precipitation is larger than the effect of other stressors considered in this study.
- (iii) Climate change and land use change exert a joint control on sediment transport, with interactions that cannot be neglected. The extent and magnitude of land-use and land-management impacts also vary depending on the location on the river and on the sub-catchment considered and must be assessed locally.
- (iv) The proposed methodology allowed assessing the robustness of arable land reduction as a measure to control sediment transport. This measure appears effective under different climatic conditions, although with different effectiveness. This study also pointed out that their effectiveness may vary depending on the future climate outcomes, providing a quantification of how it varies across the spectrum of future climatic changes.

Acknowledgements

This study forms part of the POLL-CURB project (Changes in urbanisation and its effect on water quality and quantity from local to regional scale) which is funded by the Natural Environment Research Council under the Changing Water Cycle Programme (Grant NE/K002309/1) and the MaRIUS project (Managing the Risks, Impacts and Uncertainties of droughts and water Scarcity), which is funded by the Natural Environment Research Council (NERC) under the UK Droughts and Water Scarcity Programme (Grant NE/L010364/1). The meteorological data (precipitation and temperature) were provided by the UK Met Office. The river flow data were provided by the National River Flow Archive. The suspended sediment concentration data was provided by the Environment Agency of England and Wales and by the Centre of Ecology and Hydrology's Thames Initiative. We would like to thank two anonymous reviewers for their very valuable contributions.

References

- Aksoy, H., Kavvas, M.L., 2005. A review of hillslope and watershed scale erosion and sediment transport models. *Catena* 64, 247–271. <http://dx.doi.org/10.1016/j.catena.2005.08.008>.
- Bagnold, R.A., 1966. *An approach to the sediment transport problem from general physics*. In: Geological Survey Professional Paper 422-I. U.S. Government Printing Office, Washington, DC.
- Bangash, R.F., Passuello, A., Sánchez-Canales, M., Terrado, M., López, A., Elorza, F.J., Ziv, G., Acuña, V., Schuhmacher, M., 2013. Ecosystem services in Mediterranean river basin: climate change impact on water provisioning and erosion control. *Sci. Total Environ.* 458–460C, 246–255. <http://dx.doi.org/10.1016/j.scitotenv.2013.04.025>.
- Bastola, S., Murphy, C., Sweeney, J., 2011. The sensitivity of fluvial flood risk in Irish catchments to the range of IPCC AR4 climate change scenarios. *Sci. Total Environ.* 409, 5403–5415. <http://dx.doi.org/10.1016/j.scitotenv.2011.08.042>.
- Bloomfield, J.P., Bricker, S.H., Newell, A.J., 2011. Some relationships between lithology, basin form and hydrology: a case study from the Thames basin, UK. *Hydrol. Process.* 25, 2518–2530. <http://dx.doi.org/10.1002/hyp.8024>.
- Blöschl, G., Ardoin-Bardin, S., Bonell, M., Dorninger, M., Goodrich, D., Gutknecht, D., Matamoros, D., Merz, B., Shand, P., Szolgyai, J., 2007. At what scales do climate variability and land cover change impact on flooding and low flows? *Hydrol. Process.* 21, 1241–1247. <http://dx.doi.org/10.1002/hyp.6669>.
- Boardman, J., 2015. Extreme rainfall and its impact on cultivated landscapes with particular reference to Britain. *Earth Surf. Process. Landforms.* <http://dx.doi.org/10.1002/esp.3792>.
- Boardman, J., 2003. Soil erosion and flooding on the eastern South Downs, southern England, 1976–2001. *Trans. Inst. Brit. Geogr.* 28, 176–196. <http://dx.doi.org/10.1111/1475-5661.00086>.
- Borgomeo, E., Hall, J.W., Fung, F., Watts, G., Colquhoun, K., Lambert, C., 2014. Risk-based water resources planning: Incorporating probabilistic nonstationary climate uncertainties. *Water Resour. Res.* 50, 6850–6873. <http://dx.doi.org/10.1002/2014WR015558>.
- Bowes, M.J., Gozzard, E., Johnson, A.C., Scarlett, P.M., Roberts, C., Read, D.S., Armstrong, L.K., Harman, S.A., Wickham, H.D., 2012. Spatial and temporal changes in chlorophyll-a concentrations in the River Thames basin, UK: are phosphorus concentrations beginning to limit phytoplankton biomass? *Sci. Total Environ.* 426, 45–55. <http://dx.doi.org/10.1016/j.scitotenv.2012.02.056>.
- Brown, C., Ghile, Y., Lavery, M., Li, K., 2012. Decision scaling: linking bottom-up vulnerability analysis with climate projections in the water sector. *Water Resour. Res.* 48. <http://dx.doi.org/10.1029/2011WR01212>.
- Brown, C., Wilby, R.L., 2012. An alternate approach to assessing climate risks. *Eos. Trans. Am. Geophys. Union* 93, 401. <http://dx.doi.org/10.1029/2012EO410001>.
- Buendia, C., Bussi, G., Tuset, J., Vericat, D., Sabater, S., Palau, A., Batalla, R.J., 2015. Effects of afforestation on runoff and sediment load in an upland Mediterranean catchment. *Sci. Total Environ.* 540, 144–157. <http://dx.doi.org/10.1016/j.scitotenv.2015.07.005>.
- Burt, T., Boardman, J., Foster, I.D.L., Howden, N., 2015. More rain less soil: long-term changes in rainfall intensity with climate change. *Earth Surf. Process. Landforms.* <http://dx.doi.org/10.1002/esp.3868>.
- Bussi, G., Francés, F., Horel, E., López-Tarazón, J.A., Batalla, R.J., 2014a. Modelling the impact of climate change on sediment yield in a highly erodible Mediterranean catchment. *J. Soils Sediments* 14, 1921–1937. <http://dx.doi.org/10.1007/s11368-014-0956-7>.
- Bussi, G., Francés, F., Montoya, J.J., Julien, P.Y., 2014b. Distributed sediment yield modelling: importance of initial sediment conditions. *Environ. Model. Softw.* 58, 58–70. <http://dx.doi.org/10.1016/j.envsoft.2014.04.010>.
- Bussi, G., Rodríguez-Lloveras, X., Francés, F., Benito, G., Sánchez-Moya, Y., Sopena, A., 2013. Sediment yield model implementation based on check dam inflow stratigraphy in a semiarid Mediterranean catchment. *Hydrol. Earth Syst. Sci.* 17, 3339–3354. <http://dx.doi.org/10.5194/hess-17-3339-2013>.
- Bussi, G., Whitehead, P.G., Bowes, M.J., Read, D.S., Prudhomme, C., Dadson, S.J., 2016. Impacts of climate change, land-use change and phosphorus reduction on phytoplankton in the River Thames (UK). *Sci. Total Environ.* <http://dx.doi.org/10.1016/j.scitotenv.2016.02.109>.
- Castellazzi, M.S., Matthews, J., Angevin, F., Sausse, C., Wood, G.A., Burgess, P.J., Brown, I., Conrad, K.F., Perry, J.N., 2010. Simulation scenarios of spatio-temporal arrangement of crops at the landscape scale. *Environ. Model. Softw.* 25, 1881–1889. <http://dx.doi.org/10.1016/j.envsoft.2010.04.006>.
- Cerdà, A., 1999. Seasonal and spatial variations in infiltration rates in badland surfaces under Mediterranean climatic conditions. *Water Resour. Res.* 35, 319–328. <http://dx.doi.org/10.1029/98WR01659>.
- Cerdà, A., 1998. Effect of climate on surface flow along a climatological gradient in Israel: a field rainfall simulation approach. *J. Arid Environ.* 38, 145–159. <http://dx.doi.org/10.1006/jare.1997.0342>.
- Cerdà, A., 1997. Seasonal changes of the infiltration rates in a Mediterranean scrubland on limestone. *J. Hydrol.* 198, 209–225. [http://dx.doi.org/10.1016/S0022-1694\(96\)03295-7](http://dx.doi.org/10.1016/S0022-1694(96)03295-7).
- Collins, A.L., Walling, D.E., 2007. Fine-grained bed sediment storage within the main channel systems of the frome and piddle catchments, Dorset, UK. *Hydrol. Process.* 21, 1448–1459. <http://dx.doi.org/10.1002/hyp.6269>.
- Coulthard, T.J., Ramírez, J., Fowler, H.J., Glenis, V., 2012. Using the UKCP09 probabilistic scenarios to model the amplified impact of climate change on drainage basin sediment yield. *Hydrol. Earth Syst. Sci.* 16, 4401–4416. <http://dx.doi.org/10.5194/hess-16-4401-2012>.
- Crooks, S., Davies, H., 2001. Assessment of land use change in the Thames catchment and its effect on the flood regime of the river. *Phys. Chem. Earth Part B Hydrol. Ocean. Atmos.* 26, 583–591. [http://dx.doi.org/10.1016/S1464-1909\(01\)00053-3](http://dx.doi.org/10.1016/S1464-1909(01)00053-3).
- Crossman, J., Whitehead, P.G., Futter, M.N., Jin, L., Shahgedanova, M., Castellazzi, M.S., Wade, A.J., 2013. The interactive responses of water quality and hydrology to changes in multiple stressors, and implications for the long-term effective management of phosphorus. *Sci. Total Environ.* 454–455, 230–244. <http://dx.doi.org/10.1016/j.scitotenv.2013.02.033>.
- De Vente, J., Poesen, J., Verstraeten, G., Govers, G., Vanmaercke, M., Van Rompaey, A., Arabkhedri, M., Boix-Fayos, C., 2013. Predicting soil erosion and sediment yield at regional scales: where do we stand? *Earth-Sci. Rev.* <http://dx.doi.org/10.1016/j.earscirev.2013.08.014>.
- Déqué, M., 2007. Frequency of precipitation and temperature extremes over France in an anthropogenic scenario: model results and statistical correction according to observed values. *Glob. Planet. Change* 57, 16–26. <http://dx.doi.org/10.1016/j.gloplacha.2006.11.030>.
- Duijings, J.J.H.M., 1986. Seasonal variation in the sediment delivery ratio of a forested drainage basin in Luxembourg. In: Hadley, R.F. (Ed.), *Drainage Basin Sediment Delivery*. IAHS Publ 159. IAHS Press, Wallingford, pp. 153–164.

- Evans, R., Collins, A.L., Foster, I.D.L., Rickson, R.J., Anthony, S.G., Brewer, T., Deeks, L., Newell-Price, J.P., Truckell, I.G., Zhang, Y., 2015. Extent, frequency and rate of water erosion of arable land in Britain – benefits and challenges for modelling. *Soil Use Manag.* <http://dx.doi.org/10.1111/sum.12210>.
- Farkas, C., Beldring, S., Bechmann, M., Deelstra, J., 2013. Soil erosion and phosphorus losses under variable land use as simulated by the INCA-P model. *Soil Use Manag.* 29, 124–137. <http://dx.doi.org/10.1111/j.1475-2743.2012.00430.x>.
- Foster, I.D.L., Rowntree, K.M., Boardman, J., Mighall, T.M., 2012. Changing sediment yield and sediment dynamics in the Karoo uplands, South Africa; post-European impacts. *Land Degr. Dev.* 23, 508–522. <http://dx.doi.org/10.1002/ldr.2180>.
- Fowler, H.J., Cooley, D., Sain, S.R., Thurston, M., 2010. Detecting change in UK extreme precipitation using results from the climateprediction.net BBC climate change experiment. *Extremes* 13, 241–267. <http://dx.doi.org/10.1007/s10687-010-0101-y>.
- Fowler, H.J., Ekström, M., 2009. Multi-model ensemble estimates of climate change impacts on UK seasonal precipitation extremes. *Int. J. Climatol.* 29, 385–416. <http://dx.doi.org/10.1002/joc.1827>.
- Francipane, A., Faticchi, S., Ivanov, V.Y., Noto, L.V., 2015. Stochastic assessment of climate impacts on hydrology and geomorphology of semi-arid headwater basins using a physically based model. *J. Geophys. Res. Earth Surf.* 120, 507–533. <http://dx.doi.org/10.1002/2014JF003232>.
- Fronzek, S., Carter, T.R., Luoto, M., 2011. Evaluating sources of uncertainty in modelling the impact of probabilistic climate change on sub-arctic palaeo-records. *Nat. Hazards Earth Syst. Sci.* 11, 2981–2995. <http://dx.doi.org/10.5194/nhess-11-2981-2011>.
- Fuller, R.M., Smith, G.M., Sanderson, J.M., Hill, R.A., Thomson, A.G., 2002. The UK Land Cover Map 2000: construction of a parcel-based vector map from satellite images. *Cartogr. J.* 39, 15–25.
- Futter, M.N., Butterfield, D., Cosby, B.J., Dillon, P.J., Wade, A.J., Whitehead, P.G., 2007. Modeling the mechanisms that control in-stream dissolved organic carbon dynamics in upland and forested catchments. *Water Resour. Res.* 43. <http://dx.doi.org/10.1029/2006WR004960>.
- Futter, M.N., Erlandsson, M.A., Butterfield, D., Whitehead, P.G., Oni, S.K., Wade, A.J., 2014. PERSIST: a flexible rainfall-runoff modelling toolkit for use with the INCA family of models. *Hydrol. Earth Syst. Sci.* 18, 855–873. <http://dx.doi.org/10.5194/hess-18-855-2014>.
- Gallart, F., Llorens, P., 2004. Observations on land cover changes and water resources in the headwaters of the Ebro catchment, Iberian Peninsula. *Phys. Chem. Earth* 29, 769–773. <http://dx.doi.org/10.1016/j.pce.2004.05.004>.
- Glenis, V., Pinamonti, V., Hall, J., Kilsby, C., 2015. A transient stochastic weather generator incorporating climate model uncertainty. *Adv. Water Resour.* <http://dx.doi.org/10.1016/j.advwatres.2015.08.002>.
- González-Hidalgo, J.C., Batalla, R.J., Cerdà, A., 2013. Catchment size and contribution of the largest daily events to suspended sediment load on a continental scale. *Catena* 102, 40–45. <http://dx.doi.org/10.1016/j.catena.2010.10.011>.
- González-Hidalgo, J.C., Batalla, R.J., Cerdà, A., de Luis, M., 2010. Contribution of the largest events to suspended sediment transport across the USA. *Land Degr. Dev.* 21, 83–91. <http://dx.doi.org/10.1002/ldr.897>.
- Gordon, C., Cooper, C., Senior, C.A., Banks, H., Gregory, J.M., Johns, T.C., Mitchell, J.F.B., Wood, R.A., 2000. The simulation of SST, sea ice extents and ocean heat transports in a version of the Hadley Centre coupled model without flux adjustments. *Clim. Dyn.* 16, 147–168. <http://dx.doi.org/10.1007/s003820050010>.
- Haines-Young, R., Paterson, J., Patschin, M., Wilson, A., Kass, G., 2014. The UK NEA scenarios: development of storylines and analysis of outcomes. In: Albon, S., Turner, K., Watson, R. (Eds.), *UK National Ecosystem Assessment*. UNEP, pp. 1195–1264.
- Hay, L.E., Wilby, R.L., Leavesley, G.H., 2000. A comparison of delta change and downscaled GCM scenarios for three mountainous basins in the United States. *JAWRA J. Am. Water Resour. Assoc.* 36, 387–397. <http://dx.doi.org/10.1111/j.1752-1688.2000.tb04276.x>.
- Howden, N.J.K., Burt, T.P., Worrall, F., Mathias, S.A., Whelan, M.J., 2013. Farming for water quality: balancing food security and nitrate pollution in UK river basins. *Ann. Assoc. Am. Geogr.* 103, 397–407. <http://dx.doi.org/10.1080/00045608.2013.754672>.
- Ito, A., 2007. Simulated impacts of climate and land-cover change on soil erosion and implication for the carbon cycle, 1901–2100. *Geophys. Res. Lett.* 34, 1–5. <http://dx.doi.org/10.1029/2007GL029342>.
- Jackson-Blake, L.A., Starrfelt, J., 2015. Do higher data frequency and Bayesian auto-calibration lead to better model calibration? Insights from an application of INCA-P, a process-based river phosphorus model. *J. Hydrol.* 527, 641–655. <http://dx.doi.org/10.1016/j.jhydrol.2015.05.001>.
- Jarritt, N.P., Lawrence, D.S.L., 2007. Fine sediment delivery and transfer in lowland catchments: modelling suspended sediment concentrations in response to hydrological forcing. *Hydrol. Process.* 21, 2729–2744. <http://dx.doi.org/10.1002/hyp.6402>.
- Jarritt, N.P., Lawrence, D.S.L., 2006. Simulating fine sediment delivery in lowland catchments: model development and application of INCA-Sed. In: Owens, P.N., Collins, A.J. (Eds.), *Soil Erosion and Sediment Redistribution in River Catchments: Measurement Measurement: Modelling and Management*. CAB International, pp. 207–216.
- Jin, L., Whitehead, P.G., Futter, M.N., Lu, Z., 2012. Modelling the impacts of climate change on flow and nitrate in the River Thames: assessing potential adaptation strategies. *Hydrol. Res.* 43, 902–916. <http://dx.doi.org/10.2166/nh.2011.080>.
- Julien, P.Y., 2010. *Erosion and Sedimentation*, 2nd ed. Cambridge University Press.
- Julien, P.Y., Simons, D.B., 1985. Sediment transport capacity of overland flow. *Trans. ASAE*.
- Kinniburgh, J.H., Barnett, M., 2009. Orthophosphate concentrations in the River Thames: reductions in the past decade. *Water Environ. J.* 24, 107–115. <http://dx.doi.org/10.1111/j.1747-6593.2008.00161.x>.
- Kirkby, M.J., Irvine, B.J., Jones, R.J.A., Govers, G., 2008. The PESERA coarse scale erosion model for Europe. I-Model rationale and implementation. *Eur. J. Soil Sci.* 59, 1293–1306. <http://dx.doi.org/10.1111/j.1365-2389.2008.01072.x>.
- Lázár, A.N., Butterfield, D., Futter, M.N., Rankinen, K., Thouvenot-Korppoo, M., Jarritt, N.P., Lawrence, D.S.L., Wade, A.J., Whitehead, P.G., 2010. An assessment of the fine sediment dynamics in an upland river system: INCA-Sed modifications and implications for fisheries. *Sci. Total Environ.* 408, 2555–2566. <http://dx.doi.org/10.1016/j.scitotenv.2010.02.030>.
- López-Tarazón, J.A., Batalla, R.J., Vericat, D., 2011. In-channel sediment storage in a highly erodible catchment: the River Isábena (Ebro Basin, Southern Pyrenees). *Z. Geomorphol.* 55, 365–382. <http://dx.doi.org/10.1127/0372-8854/2011/0045>.
- Lu, Q., Futter, M.N., Nizzetto, L., Bussi, G., Jürgens, M.D., Whitehead, P., 2016. Fate and transport of polychlorinated biphenyls (PCBs) in the River Thames catchment – insights from a coupled multimedia fate and hydrobiogeochemical transport model. *Sci. Total Environ.* <http://dx.doi.org/10.1016/j.scitotenv.2016.03.029>.
- Met Office, 2012. *Met Office Integrated Data Archive System (MIDAS) Land and Marine Surface Stations Data (1853–Current)*. NCAS British Atmospheric Data Centre.
- Moriassi, D.N., Arnold, J.G., Van Liew, M.W., Bingner, R.L., Harme, R.D., Veith, T.L., 2007. Model evaluation guidelines for systematic quantification of accuracy in watershed simulations. *Trans. ASAE* 50, 885–900.
- Mouri, G., 2015. Assessment of spatiotemporal variations in the fluvial wash-load component in the 21st century with regard to GCM climate change scenarios. *Sci. Total Environ.* 533, 238–246. <http://dx.doi.org/10.1016/j.scitotenv.2015.06.118>.
- Mullan, D., 2013. Soil erosion under the impacts of future climate change: Assessing the statistical significance of future changes and the potential on-site and off-site problems. *Catena* 109, 234–246. <http://dx.doi.org/10.1016/j.catena.2013.03.007>.
- Mullan, D., Favis-Mortlock, D., Fealy, R., 2012. Addressing key limitations associated with modelling soil erosion under the impacts of future climate change. *Agric. For. Meteorol.* 156, 18–30. <http://dx.doi.org/10.1016/j.agrformet.2011.12.004>.
- Murphy, J.M., Booth, B.B.B., Collins, M., Harris, G.R., Sexton, D.M.H., Webb, M.J., 2007. A methodology for probabilistic predictions of regional climate change from perturbed physics ensembles. *Philos. Trans. A. Math. Phys. Eng. Sci.* 365, 1993–2028. <http://dx.doi.org/10.1098/rsta.2007.2077>.
- Murphy, J.M., Sexton, D.M.H., Jenkins, G.J., Booth, B.B.B., Brown, C.C., Clark, R.T., Collins, M., Harris, G.R., Kendon, E.J., Betts, R.A., Brown, S.J., Humphrey, K.A., McCarthy, M.P., McDonald, R.E., Stephens, A., Wallace, C., Warren, R., Wilby, R.L., Wood, R.A., 2009. *UK Climate Projections Science Report. Climate Change Projections*. Met Office Hadley Centre, Exeter.
- Nash, J.E., Sutcliffe, J.V., 1970. River flow forecast through conceptual models – Part 1 – A discussion of principles. *J. Hydrol.* 10, 282–290. [http://dx.doi.org/10.1016/0022-1694\(70\)90255-6](http://dx.doi.org/10.1016/0022-1694(70)90255-6).
- Neal, C., Neal, M., Leeks, G.J.L., Old, G.H., Hill, L.K., Wickham, H.D., 2006. Suspended sediment and particulate phosphorus in surface waters of the upper Thames Basin, UK. *J. Hydrol.* 330, 142–154. <http://dx.doi.org/10.1016/j.jhydrol.2006.04.016>.
- Nearing, M.A., Jetten, V., Baffaut, C., Cerdan, O., Couturier, A., Hernandez, M., Le Bissonnais, Y., Nichols, M.H., Nunes, J.P., Renschler, C.S., Souchère, V., van Oost, K., 2005. Modeling response of soil erosion and runoff to changes in precipitation and cover. *Catena* 61, 131–154. <http://dx.doi.org/10.1016/j.catena.2005.03.007>.
- Nearing, M.A., Pruski, F.F., O'Neill, M.R., 2004. Expected climate change impacts on soil erosion rates: a review. *J. Soil Water Conserv.* 59, 43–50.
- Nizzetto, L., Bussi, G., Futter, M.N., Butterfield, D., Whitehead, P.G., 2016. A theoretical assessment of microplastic transport in river catchments and their retention by soils and river sediments. *Environ. Sci. Process. Impacts.* <http://dx.doi.org/10.1039/C6EM00206D>.
- Nunes, J.P., Seixas, J., Keizer, J.J., Ferreira, A.J.D., 2009. Sensitivity of runoff and soil erosion to climate change in two Mediterranean watersheds. Part II: Assessing impacts from changes in storm rainfall, soil moisture and vegetation cover. *Hydrol. Process.* 23, 1212–1220. <http://dx.doi.org/10.1002/hyp.7250>.
- Palmer, T.N., Räisänen, J., 2002. Quantifying the risk of extreme seasonal precipitation events in a changing climate. *Nature* 415, 512–514. <http://dx.doi.org/10.1038/415512a>.
- Paroissien, J.-B., Darboux, F., Couturier, A., Devillers, B., Mouillot, F., Raclot, D., Le Bissonnais, Y., 2015. A method for modeling the effects of climate and land use changes on erosion and sustainability of soil in a Mediterranean watershed (Languedoc, France). *J. Environ. Manage.* 150, 57–68. <http://dx.doi.org/10.1016/j.jenvman.2014.10.034>.
- Peizhen, Z., Molnár, P., Downs, W.R., 2001. Increased sedimentation rates and grain sizes 2–4 Myr ago due to the influence of climate change on erosion rates. *Nature* 410, 891–897. <http://dx.doi.org/10.1038/35073504>.
- Piqué, G., López-Tarazón, J.A., Batalla, R.J., 2014. Variability of in-channel sediment storage in a river draining highly erodible areas (the Isábena, Ebro Basin). *J. Soils Sediments* 14, 2031–2044. <http://dx.doi.org/10.1007/s11368-014-0957-6>.
- Poff, N.L., Brown, C.M., Grantham, T.E., Matthews, J.H., Palmer, M.A., Spence, C.M., Wilby, R.L., Haasnoot, M., Mendoza, G.F., Dominique, K.C., Baeza, A., 2015.

- Sustainable water management under future uncertainty with eco-engineering decision scaling. *Nat. Clim. Change* 1–10. <http://dx.doi.org/10.1038/nclimate2765>.
- Prudhomme, C., Crooks, S., Kay, A.L., Reynard, N., 2013. Climate change and river flooding: Part 1 classifying the sensitivity of British catchments. *Clim. Change* 119, 933–948. <http://dx.doi.org/10.1007/s10584-013-0748-x>.
- Prudhomme, C., Sauquet, E., Watts, G., 2015. Low flow response surfaces for drought decision support: a case study from the UK. *J. Extrem. Events* 2. <http://dx.doi.org/10.1142/S2345737615500050>.
- Prudhomme, C., Wilby, R.L., Crooks, S., Kay, A.L., Reynard, N.S., 2010. Scenario-neutral approach to climate change impact studies: application to flood risk. *J. Hydrol.* 390, 198–209. <http://dx.doi.org/10.1016/j.jhydrol.2010.06.043>.
- Pruski, F.F., Nearing, M.A., 2002. Climate-induced changes in erosion during the 21st century for eight U.S. locations. *Water Resour. Res.* 38. <http://dx.doi.org/10.1029/2001WR000493>, 34–11.
- Rankinen, K., Thouvenot-Korppoo, M., Lazar, A., Lawrence, D.S.L., Butterfield, D., Veijalainen, N., Huttunen, I., Lepistö, A., 2010. Application of catchment scale sediment delivery model INCA-Sed to four small study catchments in Finland. *Catena* 83, 64–75. <http://dx.doi.org/10.1016/j.catena.2010.07.005>.
- Rodríguez-Lloveras, X., Bussi, G., Francés, F., Rodríguez-Caballero, E., Solé-Benet, A., Calle, M., Benito, G., 2015. Patterns of runoff and sediment production in response to land-use changes in an ungauged catchment. *J. Hydrol.* 531, 1054–1066. <http://dx.doi.org/10.1016/j.jhydrol.2015.11.014>.
- Rodríguez-Lloveras, X., Buytaert, W., Benito, G., 2016. Land use can offset climate change induced increases in erosion in Mediterranean watersheds. *Catena* 143, 244–255. <http://dx.doi.org/10.1016/j.catena.2016.04.012>.
- Routschek, A., Schmidt, J., Krienkamp, F., 2014. Impact of climate change on soil erosion – a high-resolution projection on catchment scale until 2100 in Saxony/Germany. *Catena* 121, 99–109. <http://dx.doi.org/10.1016/j.catena.2014.04.019>.
- Serpa, D., Nunes, J.P., Santos, J., Sampaio, E., Jacinto, R., Veiga, S., Lima, J.C., Moreira, M., Corte-Real, J., Keizer, J.J., Abrantes, N., 2015. Impacts of climate and land use changes on the hydrological and erosion processes of two contrasting Mediterranean catchments. *Sci. Total Environ.* 538, 64–77. <http://dx.doi.org/10.1016/j.scitotenv.2015.08.033>.
- Simonneaux, V., Cheggour, A., Deschamps, C., Mouillot, F., Cerdan, O., Le Bissonnais, Y., 2015. Land use and climate change effects on soil erosion in a semi-arid mountainous watershed (High Atlas, Morocco). *J. Arid Environ.* 122, 64–75. <http://dx.doi.org/10.1016/j.jaridenv.2015.06.002>.
- Singh, R., Wagener, T., Crane, R., Mann, M.E., Ning, L., 2014. A vulnerability driven approach to identify adverse climate and land use change combinations for critical hydrologic indicator thresholds: application to a watershed in Pennsylvania, USA. *Water Resour. Res.* 50, 3409–3427. <http://dx.doi.org/10.1002/2013WR014988>.
- Smith, A., 2013. User Guide for the BGS DiGMapGB-50 data (V7). British Geological Survey Open Report, OR/13/008.
- Smith, G., Beare, M., Boyd, M., Downs, T., Gregory, M., Morton, D., Brown, N., Thomson, A.G., 2007. UK land cover map production through the generalisation of OS MasterMap®. *Cartogr. J.* 44, 276–283. <http://dx.doi.org/10.1179/000870407X241827>.
- Spear, R.C., Hornberger, G.M., 1980. Eutrophication in peel inlet—II. Identification of critical uncertainties via generalized sensitivity analysis. *Water Res.* 14, 43–49. [http://dx.doi.org/10.1016/0043-1354\(80\)90040-8](http://dx.doi.org/10.1016/0043-1354(80)90040-8).
- Turner, B.L., Lambin, E.F., Reenberg, A., 2007. The emergence of land change science for global environmental change and sustainability. *Proc. Natl. Acad. Sci. U.S.A.* 104, 20666–20671. <http://dx.doi.org/10.1073/pnas.0704119104>.
- Wade, A.J., Durand, P., Beaujouan, V., Wessel, W., Raat, K.J., Whitehead, P.G., Butterfield, D., Rankinen, K., Lepistö, A., 2002a. A nitrogen model for European catchments: INCA, new model structure and equations. *Hydrol. Earth Syst. Sci.* 6, 559–582. <http://dx.doi.org/10.5194/hess-6-559-2002>.
- Wade, A.J., Whitehead, P.G., Butterfield, D., 2002b. The Integrated Catchments model of Phosphorus dynamics (INCA-P), a new approach for multiple source assessment in heterogeneous river systems: model structure and equations. *Hydrol. Earth Syst. Sci.* <http://dx.doi.org/10.5194/hess-6-583-2002>.
- Wetterhall, F., Graham, L.P., Andréasson, J., Rosberg, J., Yang, W., 2011. Using ensemble climate projections to assess probabilistic hydrological change in the Nordic region. *Nat. Hazards Earth Syst. Sci.* 11, 2295–2306. <http://dx.doi.org/10.5194/nhess-11-2295-2011>.
- Whitehead, P.G., Bussi, G., Bowes, M.J., Read, D.S., Hutchins, M.G., Elliott, J.A., Dadson, S.J., 2015a. Dynamic modelling of multiple phytoplankton groups in rivers with an application to the Thames river system in the UK. *Environ. Model. Softw.* 74, 75–91. <http://dx.doi.org/10.1016/j.envsoft.2015.09.010>.
- Whitehead, P.G., Crossman, J., Balana, B.B., Futter, M.N., Comber, S., Jin, L., Skuras, D., Wade, A.J., Bowes, M.J., Read, D.S., 2013. A cost-effectiveness analysis of water security and water quality: impacts of climate and land-use change on the River Thames system. *Philos. Trans. A. Math. Phys. Eng. Sci.* 371, 20120413. <http://dx.doi.org/10.1098/rsta.2012.0413>.
- Whitehead, P.G., Lázár, A.N., Futter, M.N., Pope, L., Wade, A.J., Willows, R., Burgess, C., 2010. Modelling sediment supply and transport in the River Lugg: strategies for controlling sediment loads, in: BHS Third International Symposium, Managing Consequences of a Changing Global Environment. Newcastle, pp. 1–6.
- Whitehead, P.G., Leckie, H., Rankinen, K., Butterfield, D., Futter, M.N., Bussi, G., 2015b. An INCA model for pathogens in rivers and catchments: model structure, sensitivity analysis and application to the River Thames Catchment, UK. *Sci. Total Environ.* <http://dx.doi.org/10.1016/j.scitotenv.2016.01.128>.
- Whitehead, P.G., Wilson, E., Butterfield, D., 1998a. A semi-distributed integrated nitrogen model for multiple source assessment in catchments (INCA): Part I – model structure and process equations. *Sci. Total Environ.* 210–211, 547–558. [http://dx.doi.org/10.1016/S0048-9697\(98\)00037-0](http://dx.doi.org/10.1016/S0048-9697(98)00037-0).
- Whitehead, P.G., Wilson, E., Butterfield, D., Seed, K., 1998b. A semi-distributed integrated flow and nitrogen model for multiple source assessment in catchments (INCA): Part II – application to large river basins in south Wales and eastern England. *Sci. Total Environ.* 210–211, 559–583. [http://dx.doi.org/10.1016/S0048-9697\(98\)00038-2](http://dx.doi.org/10.1016/S0048-9697(98)00038-2).
- Wolman, M.G., Miller, J.P., 1960. Magnitude and frequency of forces in geomorphic processes. *J. Geol.* 68, 54–74.
- Worrall, F., Burt, T.P., Howden, N.J.K., 2013. The flux of suspended sediment from the UK 1974 to 2010. *J. Hydrol.* 504, 29–39. <http://dx.doi.org/10.1016/j.jhydrol.2013.09.012>.
- Zhao, G., Mu, X., Wen, Z., Wang, F., Gao, P., 2013. Soil erosion, conservation and eco-environment changes in the Loess Plateau of China. *Land Degrad. Dev.* 24, 499–510. <http://dx.doi.org/10.1002/ldr.2246>.